nature reviews chemistry

https://doi.org/10.1038/s41570-024-00652-9

Review article

Check for updates

Accessing monomers from lignin through carbon–carbon bond cleavage

Chad T. Palumbo[1], Erik T. Ouellette[1], Jie Zhu[2], Yuriy Román-Leshkov[2] ✉, Shannon S. Stahl[3] ✉ & Gregg T. Beckham[1,4] ✉

Abstract

Lignin, the heterogeneous aromatic macromolecule found in the cell walls of vascular plants, is an abundant feedstock for the production of biochemicals and biofuels. Many valorization schemes rely on lignin depolymerization, with decades of research focused on accessing monomers through C–O bond cleavage, given the abundance of β–O–4 bonds in lignin and the large number of available C–O bond cleavage strategies. Monomer yields are, however, invariably lower than desired, owing to the presence of recalcitrant C–C bonds whose selective cleavage remains a major challenge in catalysis. In this Review, we highlight lignin C–C cleavage reactions, including those of linkages arising from biosynthesis (β–1, β–5, β–β and 5–5) and industrial processing (5–CH_2–5 and α–5). We examine multiple approaches to C–C cleavage, including homogeneous and heterogeneous catalysis, photocatalysis and biocatalysis, to identify promising strategies for further research and provide guidelines for definitive measurements of lignin C–C bond cleavage.

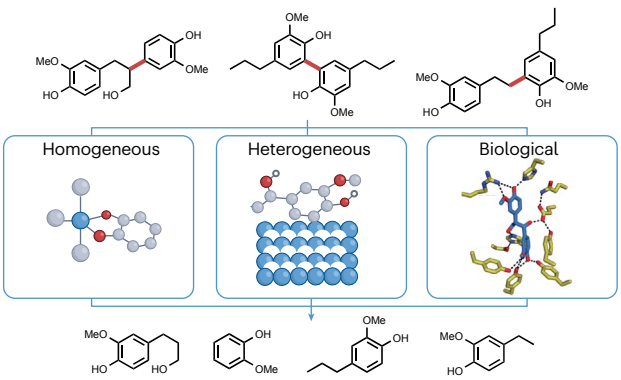

Sections

[1]Renewable Resources and Enabling Sciences Center, National Renewable Energy Laboratory, Golden, CO, USA. [2]Department of Chemical Engineering, Massachusetts Institute of Technology, Cambridge, MA, USA. [3]Department of Chemistry. Great Lakes Bioenergy Research Center, University of Wisconsin-Madison, Madison, WI, USA. [4]Center for Bioenergy Innovation, Oak Ridge, TN, USA. ✉e-mail: yroman@mit.edu; stahl@chem.wisc.edu; gregg.beckham@nrel.gov

Introduction

Lignin is a heterogeneous macromolecule found in the cell walls of vascular plants that comprises methoxylated phenyl propane units linked through various carbon–carbon (C–C) and carbon–oxygen (C–O) bonds. It makes up 15–35% of lignocellulosic biomass[1] and is produced by enzyme-mediated oxidative polymerization of monolignol building blocks from the shikimate pathway, including the three canonical hydroxycinnamyl monolignols – that is, *p*-coumaryl (H-type), *p*-coniferyl (G-type) and *p*-sinapyl (S-type) alcohols (Supplementary Fig. 1a) – along with intermediates from the monolignol biosynthesis pathway and numerous derivatives[2,3]. Lignin structure can be further modified by the incorporation of flavonoids and stilbenoids[2,3]. The structure and quantity of lignin depend on factors including the species, season and environmental stressors[4,5]. This inherent variability, combined with its propensity for condensation reactions forming recalcitrant C–C bonds during biomass processing, complicates lignin valorization – particularly its conversion to useful monomers. Of the more than 50 million tons of lignin extracted annually from the pulp and paper industry, only 2% is used for commercial applications, largely as polymeric lignosulfonates[6], whereas the rest is burned for energy reclamation or consumed for process chemicals regeneration. Burning lignin is a highly polluting process, and it causes numerous air quality issues in the vicinity of the biorefinery[7].

Rigorous process analyses have shown that lignin valorization – beyond heat and power generation – is critical for a bioeconomy based on the use of lignocellulose for biofuels and biochemicals[7–9]. Today, lignin depolymerization to phenolic monomers represents one of the most sought-after approaches to derive value from lignin[10–16], and many strategies have been developed to cleave the abundant β–O–4 linkage. Considerable progress has resulted in processes able to selectively cleave ether linkages through reduction[17,18], oxidation[19,20], stabilization chemistry[16,21,22] and many other strategies[10–16]. At present, achieving near-theoretical ether bond cleavage in lignin to monomers is tractable[12,13].

Despite the abundance of ether bonds in lignin, achieving high phenolic monomer yields through most deconstruction strategies is inherently limited owing to the presence of C–C bonds[10,23]. This challenge has garnered increased attention[24], with developments in homogeneous thermal catalysis[25], photocatalysis[26,27] and cracking reactions in heterogeneous systems[28,29]. To date, however, there remain limited options for this transformation, prompting the development of new and robust approaches for lignin C–C bond cleavage. Although C–C bond activation in general has been reviewed extensively[30–37], there are only a few examples that are relevant to cleaving C–C bonds in lignin[27,36,38–40]. Furthermore, most lignin-related studies are performed on model compounds, leaving it unclear how the process compares with that of a true-lignin substrate.

Here, we review lignin C–C bond cleavage research, highlighting studies that systematically target C–C bonds, paying special attention to those that utilize monomer-free substrates and benchmark yields against those of established C–O cleavage methods. We start by identifying the types of C–C bonds present in both native and processed lignins, providing perspective into the challenges of C–C cleavage and the dependence of the lignin source. We then highlight recent reports of C–C bond cleavage of lignin substrates or model compounds for monomer production, classifying these approaches into specific strategies. Finally, we discuss the effectiveness of various state-of-the-art C–C bond cleavage methods and provide insight into future opportunities in this area.

Lignin C–C bonds formed during biosynthesis

Besides aryl–ether linkages, there are several C–C bonds produced when lignin is formed in planta that contribute to its recalcitrance. During lignin biosynthesis, three primary monolignols (coumaryl alcohol (H), coniferyl alcohol (G) and sinapyl alcohol (S); Supplementary Fig. 1a) are synthesized from aromatic amino acid intermediates before being transported to the cell wall, where they deposit at nucleation sites, largely after deposition of cellulose and hemicellulose in the inner layer of the secondary wall[23,41]. Lignification occurs with the aid of laccases and peroxidases, which abstract hydrogen from phenolic hydroxyl groups of the monolignols to generate resonance-stabilized phenoxyl radicals. The unpaired electrons, localized at the 'β', the 'O4' and the '5' positions of each aromatic unit (Supplementary Fig. 1b), couple in a combinatorial fashion to form the lignin polymer (Fig. 1a). Common C–O linkages include the β–O–4 and 4–O–5 bonds (Fig. 1a and Supplementary Fig. 1c), whereas common C–C linkages are β–1, β–5, β–β and 5–5 bonds (Fig. 1a and Supplementary Fig. 1d).

The β–O–4 linkage is by far the most common of native lignin linkages, and it is found in large percentages in all lignin feedstocks (~30–36% in softwoods and ~55–60% in hardwoods). Given the prevalence of β–O–4 bonds and the historical focus on cleavage of these relatively labile ether bonds, the theoretical maximum monomer yield from lignin has commonly been represented throughout the literature as x^2, in which x is the percentage of β–O–4 bonds present; therefore, theoretical monomer yields from softwoods and hardwoods, respectively, are ~10–15% and ~36% through ether bond cleavage alone[42–44]. By contrast, C–C linkages are found in lower percentages and their distribution depends on numerous factors, including the ratio of S/G units, electronic effects arising from ring substitution[45,46] and monolignol concentrations during lignification[47–49]. Studies on in vitro lignin biosynthesis and computational analyses have examined the impact of these parameters on C–C bond quantity and distribution[50,51]. The S/G ratio is an important factor in C–C bond formation given that S units lack an open '5' position, thus preventing the formation of β–5-type or 5–5-type linkages in favour of β–1 and β–β bonds (in addition to β–O–4). Given that the S/G ratio is feedstock-dependent – for example, softwoods primarily contain G-type units[52] whereas the S/G ratios in natural poplar populations vary between <1 and >3, and genetically modified variants can display even greater S/G ratios[53] – the feedstock greatly influences the relative distributions of C–C bonds[54]. Monolignol concentrations during lignification also impact the formation of C–C linkages relative to others. For example, in vitro lignification using *p*-hydroxycinnamyl alcohol precursors demonstrated that high monolignol concentrations favour rapid C–C bond formation, predominantly via radical β–β and β–5 coupling[45,48], whereas gradual monolignol introduction produced lignin with 50% β–O–4-linked dimers.

Lignin C–C bonds through processing

There is more than a century's worth of literature describing methods to extract lignin from plants, and the conditions used therein substantially alter lignin's structure. Lignin-first methods, which solubilize lignin directly from native lignocellulosic biomass, are notable for minimizing condensation reactions. These methods use active stabilization strategies, such as hydrogenolysis and hydrogenation, thereby targeting reactive functional groups that would otherwise lead to new C–C linkages[55]. After work-up, a soluble lignin oil is obtained with a structure resembling that in Fig. 1b, which contains 35–50 wt% monomers. These monomers are mainly produced through reductive cleavage of C–O bonds. The remaining lignin aromatics are found in

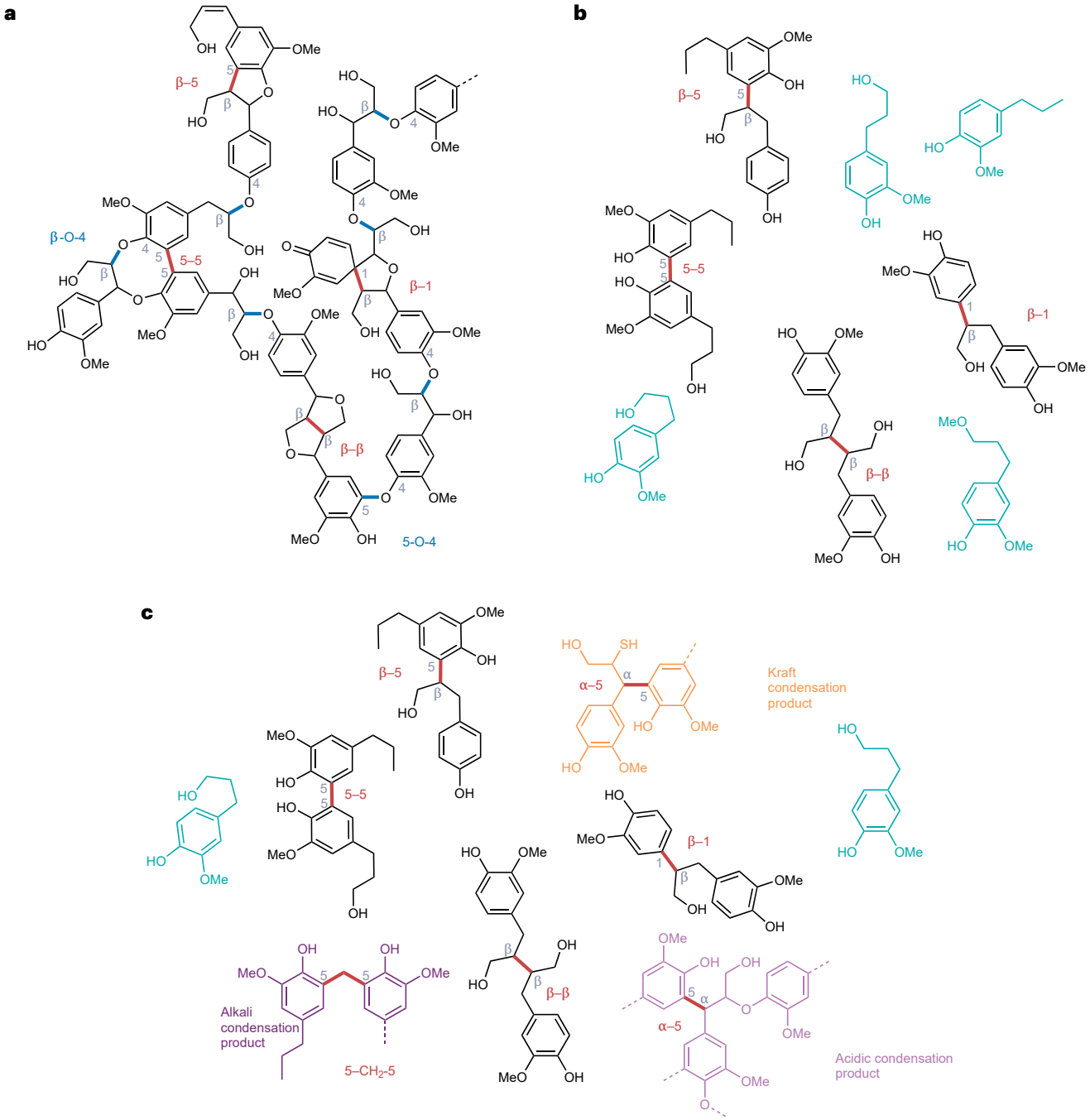

Fig. 1 | Lignin structures and common linkages. a, Representative lignin structures and major linkage types in native lignin. **b**, 'Lignin-first' monomers and dimers produced via reductive catalytic fractionation[52]. **c**, Post-processed lignin monomers and oligomers from alkali, acidic and/or kraft treatments, highlighting new C–C bonds introduced via condensation reactions and incorporation of sulfur via kraft treatment. C–O linkages are represented by blue bonds, C–C linkages by red bonds, and monomers are reported in green. Dashed lines represent additional, unspecified linkages to the larger polymer.

dimers and oligomers primarily bound through four main C–C bonds: β–5, β–β, 5–5 and β–1 (ref. 52) (Fig. 1b).

Other fractionation methods afford highly degraded and structurally complex lignin products. The widely used kraft process[56] produces a nearly pure holocellulose pulp and a highly degraded lignin coproduct. This is achieved by heating biomass with sodium sulfide and sodium hydroxide, leading to the dissolution of lignin and hemicellulose, and facilitating their separation[57,58]. The structural complexity of kraft lignin can be described by the reactivity of both phenolic and non-phenolic lignin units, which are subject to condensation reactivity under alkaline

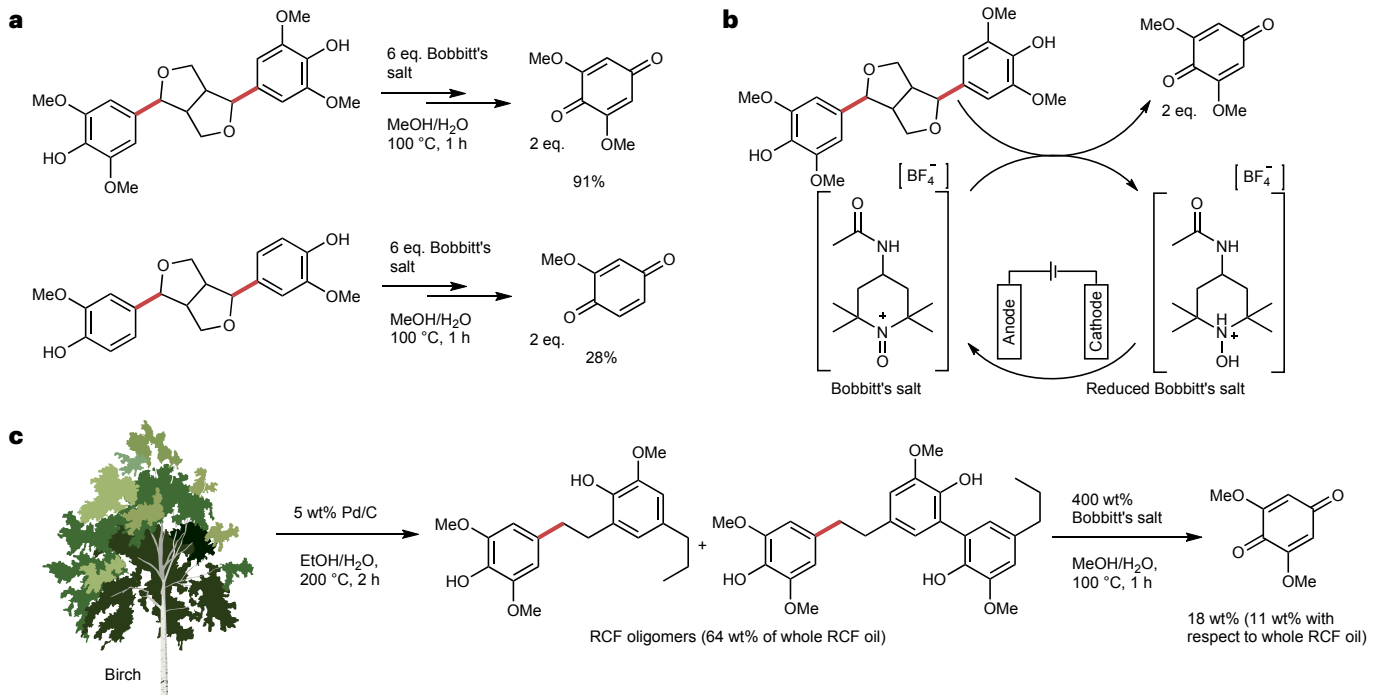

Fig. 2 | Oxidative C–C cleavage through phenol activation. Illustration of the work by Subbotina et al. demonstrating oxidative cleavage of G-type (guaiacyl) and S-type (syringyl) β–β model dimers (part **a**), electrochemical regeneration of the oxidant (part **b**) and oxidation of birch wood dimers and oligomers produced through reductive catalytic fractionation (RCF) and distillation[42] (part **c**). Bonds represented in red highlight C–C cleavage points. Percent yields are reported as molar yields unless specifically stated as weight percent (wt%).

conditions (see Fig. 1c for representative products and Supplementary Fig. 2a for detailed reaction pathways)[13]. This leads to new types of bonds, including α–5 and 5–CH_2–5 (methylene), among others. The complexity of the lignin chemistry in kraft pulping is an active area of investigation[59–61], and it has been estimated that only up to 45% of the kraft lignin structure is known[61].

Under acidic conditions, which includes some sulfite pulping[57,58], organosolv processes (extractions with an organic solvent) and acid or hydrothermal pre-treatment, the hydrolysis of ether bonds between lignin and polysaccharides solubilizes the polysaccharides. In sulfite pulping and organosolv processes, lignin is also solubilized, either through addition of sulfonate groups enabling dissolution in water (sulfite pulping) or through organosolv. By contrast, certain acid pre-treatments can lead to lignin precipitation (to produce a residue known as Klason lignin). Similar to alkaline conditions, condensation reactions are observed during acidic processing but occur through different mechanisms (see Fig. 1c for representative products and Supplementary Fig. 2b for detailed reaction pathways). Both alkaline-processed and acid-processed lignins are difficult to depolymerize owing to the myriad of new C–C bonds formed.

Homogeneous C–C bond cleavage of lignin and models

Many C–C bond cleavage reactions of non-lignin organic compounds are driven by the alleviation of ring strain, the establishment of aromaticity or the formation of stable products, such as five-membered metallocycles or strong metal–C(sp^2) bonds[30–32,34,35]. However, often these chemistries cannot be applied to lignin owing to its inherent structural features, such as the presence of phenolic hydroxyl groups, which complicate many catalytic strategies. As a result, developing C–C bond cleavage strategies that also tolerate lignin's reactive functional groups is difficult.

In the following sections, we describe advances in C–C cleavage reactivity, with a focus placed on lignin and lignin model substrates, and the strategies implemented to promote C–C cleavage. We begin by discussing strategies based on homogeneous chemistry, before focusing on heterogeneous catalytic methods, photocatalytic approaches and biocatalytic cleavage reactions of lignin (admittedly, some overlap exists among the different strategies).

Oxidative C–C cleavage in phenolic lignin

The naturally occurring phenolic moieties in lignin are subject to oxidation and can interfere with oxidative processes. However, Subbotina et al. leveraged the oxidative sensitivity of phenols to promote oxidative cleavage of C–C bonds in oligomers derived from the reductive catalytic fractionation (RCF) of birch wood[42] (Fig. 2a–c). Their method used Bobbitt's salt, the oxoammonium compound derived from 4-acetamido-2,2,6,6-tetramethylpiperidine-*N*-oxyl, to produce 2,6-dimethoxybenzoquinone as the final product. They proposed a mechanism that involves the initial oxidation of the phenol hydroxyl followed by nucleophilic attack by methanol at the *para* position, and subsequent *ipso*-substitution by water. An additional oxidation step produces the quinone product via cleavage of the C_{aryl}–C_α bond. Quinone yields of up to 94 mol% with an S-type model compound and 18 wt% with birch RCF oligomer were obtained following treatment with super stoichiometric quantities of Bobbitt's salt (Fig. 2a). For the

G-type model, a substantially lower yield was observed (28 mol%), likely owing to condensation reactions at the 5-position. The oxoammonium reagent could be regenerated electrochemically and re-used to afford similar product yields (Fig. 2b). An 11 wt% quinone yield was obtained from C–C bond cleavage, when normalized with respect to the RCF oil (Fig. 2c).

Although commonly used as inhibitors for oxidative processes, the above results demonstrate that phenolic hydroxyl groups can be targeted for selective C–C bond cleavage. By choosing suitable catalysts and reaction conditions, it is also possible to activate phenolic substrates catalytically. The next few examples illustrate how transition metals, when paired with oxygen, catalytically cleave C–C bonds of phenolic substrates.

Aerobic oxidations with mid-to-late first-row transition metals

Aerobic oxidations can be performed selectively with a catalyst that activates oxygen directly, producing a transient metal–O_2 species whose reactivity and electronic structure depend on the metal and its surrounding environment. It has been shown that a Co-Schiff base catalyst activates O_2 and phenolic hydroxyl groups to cleave the C–C bond of benzylic alcohol lignin models, affording benzoquinone products[62–70] (Fig. 3a–c). Both the ligand environment and the type of substrate affect the products formed. In general, five-coordinate complexes with an N-donor ligand *trans* to the O_2 binding site, namely [bis(2-salicylideneiminopropyl)methylamine]cobalt, Co(smdpt), and [bis(salicyldiene)ethylenediamine](pyridine)cobalt, Co(salen)(py), demonstrated higher reactivity than the four-coordinate complex without a *trans* pyridine ligand Co(salen) (Fig. 3a). The axial N-donor ligand is believed to promote O_2 binding, which is needed for the reaction with the phenolic substrates[71]. The S-type substrates were more readily converted to C–C cleavage products than G-type models, an observation also made for β–O–4 models[67]. With tulip poplar organosolv lignin, 3.5 wt% of total products were isolated, comprising equimolar quantities of quinone and aldehyde/ester products[67] (Fig. 3b). Mechanistic studies by Drago et al. on the oxidation of dialkylphenols by Co(smdpt) demonstrated a first-order dependence of the cobalt catalyst, oxygen and the phenolic substrate[64] (Fig. 3c). The mechanism proposed includes an initial hydrogen atom abstraction of the phenolic hydroxyl by a cobalt–dioxygen species to generate a phenoxyl radical that couples to another equivalent of cobalt–dioxygen to form a cobalt–peroxyquinone. This species then reacts further to yield benzoquinone through C–C cleavage and an equivalent of cobalt(III) hydroxyl, which ultimately regenerates the phenoxyl radical and the Co(II) catalyst.

Attempting to compare differences in behaviour between early and late transition metals, Baker and Hanson studied the ability of homogeneous vanadium and copper catalysts to cleave the C–C bonds in non-phenolic and phenolic β–1 lignin models[25,72] (Fig. 3d). With non-phenolic substrates, the most active vanadium catalyst studied, bis(quinolate)V(O)(O^iPr), afforded products of alcohol oxidation and dehydration, whereas the CuOTf/TEMPO/2,6-lutidine system afforded C–C bond cleavage products. Kinetic and computational studies of the non-phenolic β–1 model with the vanadium catalyst suggest that the reaction proceeds through a two-electron, base-assisted pathway[72,73]. For copper, the authors proposed two possible radical pathways on the basis of the observed product distributions, including (1) primary alcohol oxidation followed by C–C cleavage through a retro-aldol reaction[74,75] and (2) one-electron oxidation of the aromatic, leading to a radical cation intermediate that undergoes C–C scission[76,77]. With phenolic substrates, both catalysts afforded C–C bond cleavage products. It was suggested that bis(quinolate)V(O)(O^iPr) promotes radical pathways, yielding 2,6-dimethoxybenzoquinone as the major product, in a similar fashion to the aforementioned cobalt chemistry described by Bozell and Drago. The selectivity of the CuOTf/TEMPO/2,6-lutidine system changed with catalyst loadings. With low Cu loadings, oxidation of the α-OH afforded only the aryl ketone product, consistent with Cu/TEMPO-catalysed aerobic oxidations[75,78–80]. C–C bond cleavage products were only observed with stoichiometric Cu/TEMPO loadings. Oxidation of extracted lignin with both catalysts demonstrated a shift to decreased molecular weights, consistent with overall lignin deconstruction, but monomer yields were not reported.

The reactivity of the Cu/O_2/nucleophile system has been studied for decades[81,82], and it has recently been applied to cleave C–C bonds in non-phenolic aryl ketone molecules. Jiao and colleagues reported the conversion of non-phenolic aryl ketones to esters, aldehydes and amides through oxidative C–C bond cleavage[83–85]. By stirring aryl ketone substrates with 10 mol% CuBr, pyridine and butanol, C–C bond cleavage is effected and produces ester and aldehyde products in 72–81% yields (Fig. 3e). The authors proposed two pathways that occur simultaneously and diverge after a common hemiketal intermediate. In one pathway, base-promoted oxidation of the hemiketal by Cu(II) yields a carbon-centred radical that couples with molecular oxygen, affording a superoxide intermediate. The superoxide intermediate is then reduced by Cu(I) and protonated, affording the hydroperoxide that undergoes C–C scission, ultimately affording the ester product and an equivalent of aldehyde. In the second pathway, the hemiketal dehydrates to form a vinyl ether intermediate, which reacts further with a Cu(II)–superoxide radical, leading to a dioxetane intermediate. This intermediate then undergoes C–C and C–O bond cleavage, ultimately producing the observed ester and aldehyde products, with the ester oxygen derived from O_2.

Jiao and colleagues[83] also showed that amide products are generated when the nucleophile is azide, although at lower yields (Supplementary Fig. 3a). Notably, this system has been used to ring-open aromatics when the proper functional groups are available for catalyst binding[85] (Supplementary Fig. 3b). More examples of copper-catalysed aerobic oxidations have been reported, and they displayed similar C–C bond cleavage reactivity[86,87].

In a different Cu-based homogeneous system, Hu and colleagues demonstrated C–C cleavage in β–O–4 and β–1 model compounds in water at pH 2 under 1 atm air at 30–50 °C with a CuCl catalyst[88] (Fig. 3f). Studies of the substrate scope demonstrated high conversion (>95%) and C–C cleavage yields up to 86%. Notably, it was shown that the reaction is effective with model compounds bearing free phenols and more complex β–O–4 models. For example, 1-(4-hydroxy-3,5-dimethoxyphenyl)-2-(2-methoxyphenyl)propane-1,3-diol underwent cleavage to produce syringaldehyde and guaiacol in 76% and 84% yield, respectively. The simple β–1 model 2-phenylacetophenone also underwent C–C scission to produce benzoic acid and benzaldehyde in 83% and 77% yield, respectively. C–C cleavage was observed only for substrates with an α-OH or α-ketone, suggesting an important role for substrate activation and cleavage of the C_α–C_β bond. The application of the system to biomass samples at 160 °C and 5 bar air with 50% catalyst loadings afforded C–C bond cleavage products in 39 wt% with eucalyptus wood and total yields in the 20–30 wt% range with corn stover, pine, bagasse, pennisetum and bamboo.

Another possibility is to leverage the diradical nature of O_2 and propagate radical chain processes via metal-catalysed autoxidation to induce C–C cleavage. Motivated by the initial results of Partenheimer and Clatworthy[89–91], who utilized the autoxidation of β–O–4-containing models and lignin for monomer production, Gu and Palumbo relied on Co-catalysed and Mn-catalysed autoxidation (using chemistry

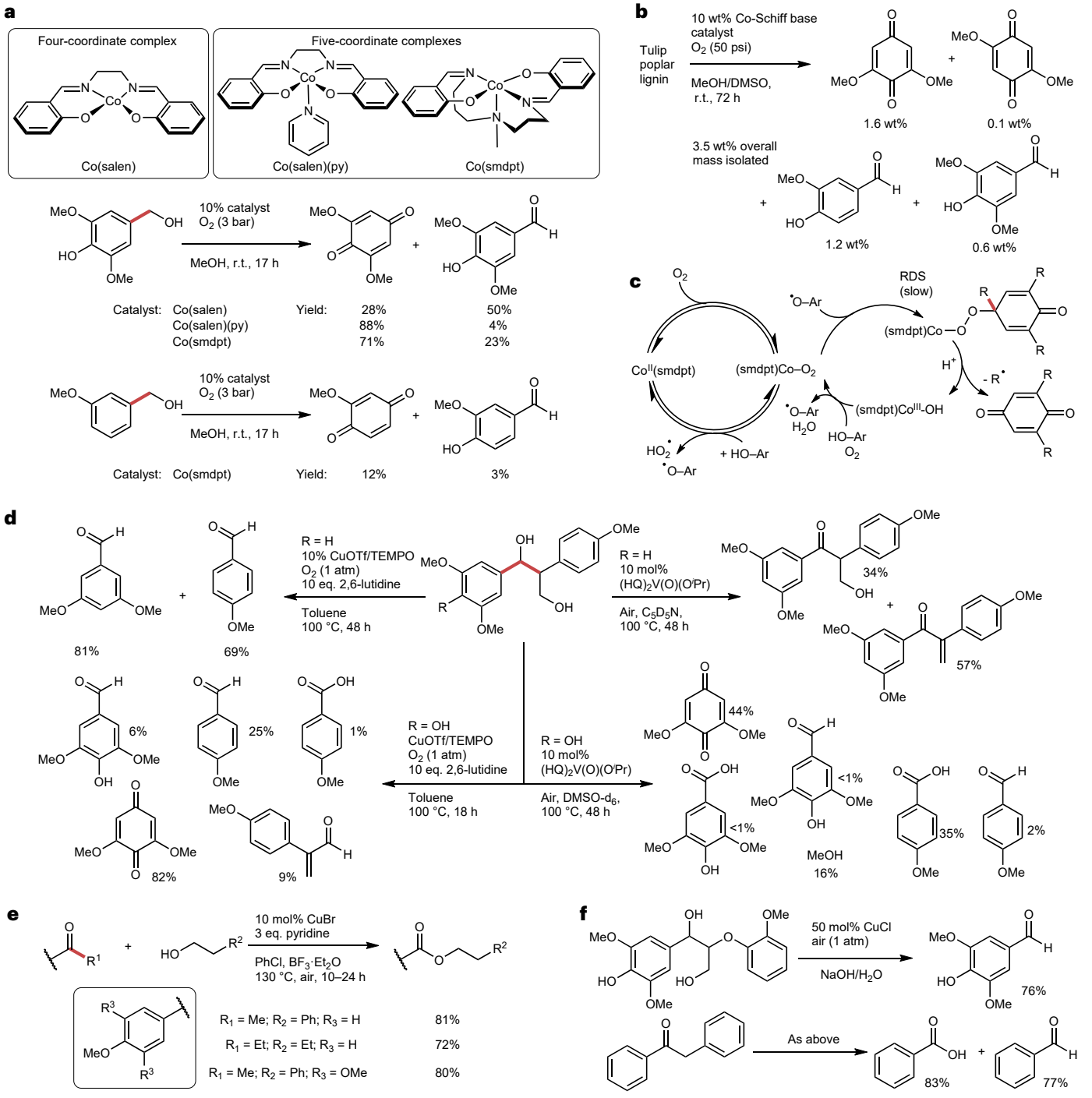

Fig. 3 | Oxidative C–C cleavage using first-row transition metals. **a**–**c**, Cobalt(salen)-mediated C–C bond cleavage showing the effects of the coordination number and substrate type[68] (part **a**), cobalt(salen)-mediated oxidation of tulip poplar lignin[67] (part **b**) and a proposed mechanism of C–C bond cleavage[64] (part **c**). **d**, Results of the studies conducted on the V-mediated and Cu-mediated oxidative C–C cleavage of non-phenolic (R = H) and phenolic (R = OH) lignin model substrates[25,72]. **e**, Copper-catalysed C–C bond cleavage via aerobic oxidation of H-type (*p*-coumaryl) and S-type (syringyl) aryl ketones to afford ester products[83,84]. **f**, Cu-catalysed C–C cleavage of β-O-4 and β-1 linkages in basic media[88]. Bonds represented in red highlight C–C cleavage points. Percent yields are reported as molar yields unless specifically stated as weight percent (wt%). HQ, quinolate; RDS, rate-determining step; r.t., room temperature.

based on the Mid-Century process to convert *p*-xylene to terephthalic acid) to cleave the C–C bonds of acetyl-protected[92] (Fig. 4a–c) and methyl-protected[93] (Fig. 4d–f) oligomers from poplar and pine RCF lignin oils. C–C bond cleavage occurs through β-scission following the thermolysis of radical intermediates in the radical chain process. With modest yields of aromatic products, oxidation of model compounds demonstrated monomer production from three of the four types of C–C bonds studied. The resulting aryl acid products are bioavailable and were catabolized by engineered strains of *Pseudomonas putida* (*P. putida*) to selectively generate a single product, *cis,cis*-muconic acid[94].

In the work by Gu et al.[92] and Palumbo et al.[93], two aerobic oxidation catalyst systems were studied: Co/Mn/Br and Mn/Zr in acetic acid. Oxidation of acetyl-protected model dimers with the Co/Mn/Br catalyst demonstrated C–C bond cleavage and monomer production with yields up to 64 mol%. Application of this chemistry to poplar oligomers afforded monomeric products in 0.24 mmol g^{-1} of oligomer substrate (13 wt%). The less active Mn/Zr catalyst, conversely, does not oxidize the acetyl-protected substrate to an appreciable extent. However, using a more resonance-donating methyl-protecting group afforded C–C bond cleavage products with monomer yields of up to 45 mol%. Application of this catalytic system to methylated pine and poplar oligomers affords total product yields of 1.0 mmol g^{-1} of oligomer substrate (20 wt%), which is similar to the yields reported by Subbotina and colleagues[42].

C–C cleavage through autoxidation is convenient as the reagents are inexpensive (air can be used as the oxidant), and the bioavailability of the products enables simplification of the product stream via catabolic processes[95,96]. Despite its benefits, the potential of autoxidation for lignin valorization would be improved by increasing reaction selectivity. Full substrate conversion with low quantities of identifiable aromatic products and the identification of products of aromatic ring opening are consistent with overoxidation and lignin degradation. The chemistry also necessitates the protection of inhibiting phenol groups.

The final example of C–C cleavage in homogeneous systems describes a method to cleave the 5–5 bond in both model compounds and softwood (spruce) RCF lignin oil.

Overcoming the kinetic barrier of 5–5 cleavage through catalyst tethering

The 5–5 bond of lignin is one of the most difficult to cleave, as it is thermodynamically strong[97,98] and kinetically difficult to access. Dong et al. demonstrated 5–5 cleavage in various models and in spruce lignin[99,100] by functionalizing phenolic lignin models with removable $^{i}Pr_2P$ metal-binding ligands (removable directing groups) (Fig. 5a). Subsequent treatment of the 5–5 model with 0.5 mol% $[Rh(C_2H_4)_2Cl]_2$ and 3.4 bar of H_2 at 150 °C gave 4-alkylguaiacol products in 56–84 mol% yield. Alternatively, the reaction could be accomplished in a single step, as shown with R = Me, to afford 4-methylguaiacol in 50 mol% yield. With spruce RCF oil (Fig. 5b), a 29 mg yield of 4-propylguaiacol was obtained through 5–5 cleavage of 40.6 mg of the dipropyl 5–5 compound in the lignin substrate, representing a yield of 70 mol%.

As evidenced by the variety of reports thus far, homogeneous reactants and catalysts have shown promise for inducing C–C cleavage in lignin models and substrates. Notably, apart from catalyst tethering for the cleavage of 5–5 bonds, the vast majority of homogeneous efforts have been based on oxidative C–C cleavage. Although the products of these oxidative strategies clearly demonstrate carbon–carbon bond cleavage of lignin substrates, the mechanisms involved are system-dependent and not always clearly defined or elucidated. There is substantial room for improving our mechanistic understanding of these oxidative processes, particularly as they relate to lignin-specific substrates. Better mechanistic rationale in this area should aid the improvement and development of new homogeneous C–C cleavage strategies.

Heterogeneous C–C bond cleavage in lignin

The use of heterogeneous catalysts offers promising strategies for efficient C–C cleavage in lignin. Heterogeneous catalysis holds distinct processing advantages, including the capability to operate under a broader range of conditions, the facile separation of catalysts from solvents and products, and the recyclability of the catalysts[24,101–103]. In the following section, we introduce additional examples and categorize different types of heterogeneous catalysts effective for lignin C–C cleavage, including metal oxides/sulfides, acidic zeolites and bifunctional catalysts.

Amorphous metal oxides and oxygen vacancies for O_2 activation

In contrast to the homogeneous Cu/O_2 systems from Huang et al.[84] and Qiu et al.[85] (Supplementary Fig. 3a,b), He and colleagues developed a robust heterogeneous reaction that also produces amide and nitrile products but avoids the use of toxic and explosive N_3^- salts. This work implicated the importance of oxygen vacancies for direct O_2 activation using an amorphous manganese oxide catalyst that promotes conversion of lignin models to amide products through C–C bond cleavage[104] (Fig. 5c). The substrate scope included primary and secondary alcohols, vicinal diols, β–O–4 models, and β–1 models, and the reaction used O_2 and NH_3 at elevated temperatures (110–160 °C). Comparisons between amorphous and crystalline manganese oxides indicated a lower average manganese oxidation state in the amorphous material, promoting oxygen vacancies in four-coordinate Mn^{3+} sites and producing a high surface area material. Density functional theory calculations were consistent with lower O_2 binding energies to the four-coordinate sites and were used to propose a reaction mechanism. By changing the solvent and temperature, C–C cleavage of the benzylic carbon was observed to yield nitrile products.

Metal sulfides for sulfur-containing technical lignins

Motivated by previous studies on FeS_2-mediated coal liquefaction[105], Shuai et al. explored the use of CoS_2 for C–C cleavage in kraft lignin and a diarylmethane model compound[106], leveraging the robustness of metal sulfides in sulfur-rich environments. When a diarylmethane model dimer was treated with catalyst in heptane at 250 °C, an 88 mol% yield was obtained for phenolic monomers, including 2-hydroxy-4-methylphenol and 2-methoxy-4-methylphenol. Prolonged reaction times led to decreased aromatic yields owing to product decomposition[106] (Fig. 6a). With kraft lignin in dioxane, they observed a 13 wt% yield of monomers and a reduction in molecular weight, whereas with heptane as a solvent, only a 1 wt% yield of monomers was observed (Fig. 6b). The CoS_2 catalyst outperformed the Ru/C catalyst under similar conditions. The extent of methylene linkage cleavage was suggested to depend on the chemical environment surrounding lignin molecules, particularly the adjacent phenolic groups that likely interact with Co^{2+} sites on cobalt sulfide. The strong electron-donating nature of these phenolic groups is expected to weaken the methylene linkage, facilitating C–C cleavage to form monomers.

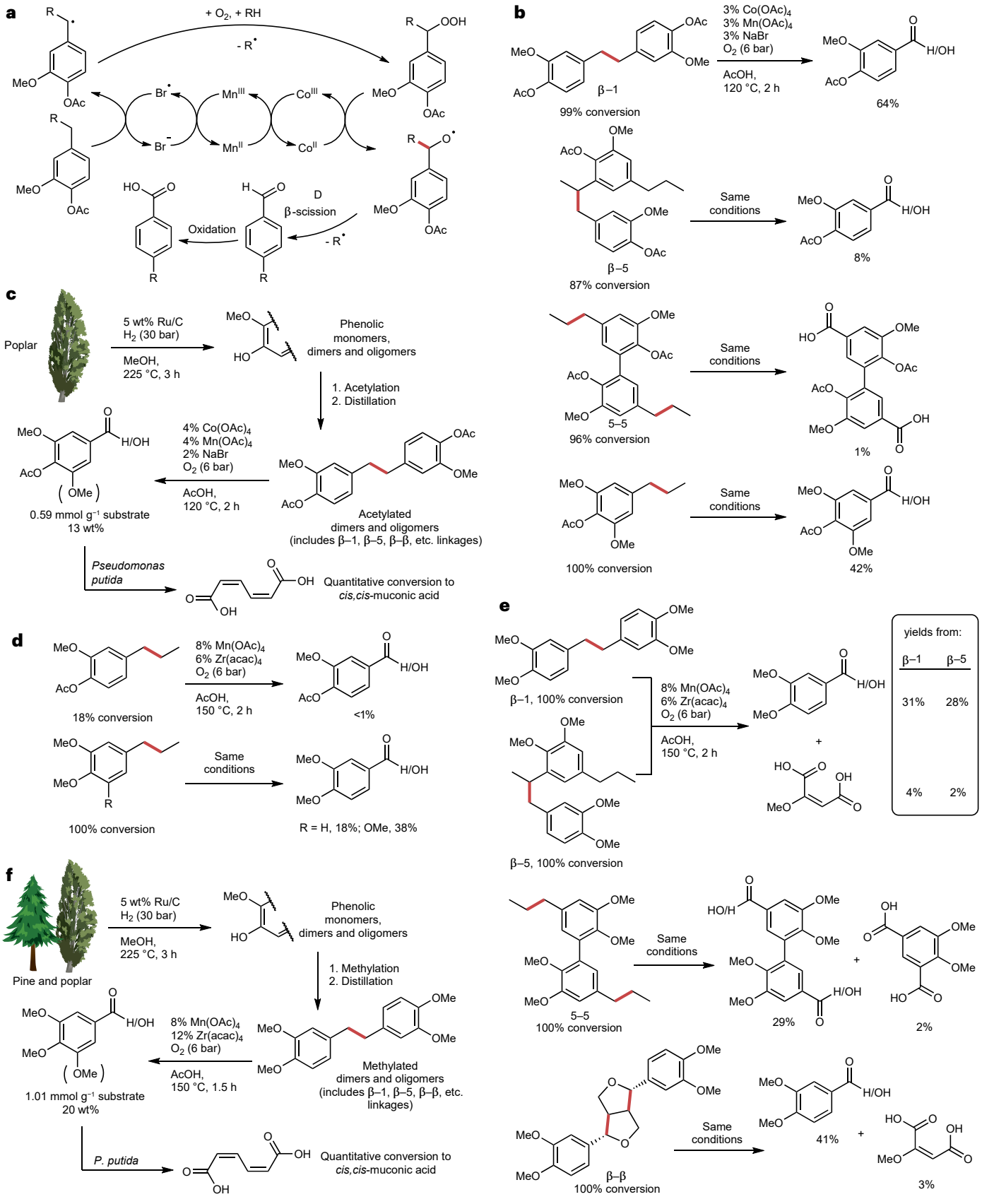
a
+ O2, + RH
- R•
Br•
Br-
MnIII
MnII
CoIII
CoII
Oxidation
D
β-scission
- R•
b
3% Co(OAc)4
3% Mn(OAc)4
3% NaBr
O2 (6 bar)
AcOH,
120 °C, 2 h
β–1
99% conversion
64%
β–5
87% conversion
Same conditions
8%
5–5
96% conversion
1%
100% conversion
42%
c
Poplar
5 wt% Ru/C
H2 (30 bar)
MeOH,
225 °C, 3 h
Phenolic monomers, dimers and oligomers
1. Acetylation
2. Distillation
4% Co(OAc)4
4% Mn(OAc)4
2% NaBr
O2 (6 bar)
AcOH,
120 °C, 2 h
0.59 mmol g−1 substrate
13 wt%
Acetylated dimers and oligomers (includes β–1, β–5, β–β, etc. linkages)
Pseudomonas putida
Quantitative conversion to cis,cis-muconic acid
d
8% Mn(OAc)4
6% Zr(acac)4
O2 (6 bar)
AcOH,
150 °C, 2 h
18% conversion
<1%
Same conditions
100% conversion
R = H, 18%; OMe, 38%
e
β–1, 100% conversion
8% Mn(OAc)4
6% Zr(acac)4
O2 (6 bar)
AcOH,
150 °C, 2 h
β–5, 100% conversion
yields from:
β–1 β–5
31% 28%
4% 2%
5–5
100% conversion
Same conditions
29%
2%
β–β
100% conversion
41%
3%
f
Pine and poplar
5 wt% Ru/C
H2 (30 bar)
MeOH,
225 °C, 3 h
Phenolic monomers, dimers and oligomers
1. Methylation
2. Distillation
8% Mn(OAc)4
12% Zr(acac)4
O2 (6 bar)
AcOH,
150 °C, 1.5 h
1.01 mmol g−1 substrate
20 wt%
Methylated dimers and oligomers (includes β–1, β–5, β–β, etc. linkages)
P. putida
Quantitative conversion to cis,cis-muconic acid

Fig. 4 | Autooxidation catalysis for lignin C–C cleavage. a, Simplified scheme of the reaction catalysed by the Mid-Century Co/Mn/Br catalyst and the relevant cleavage of C–C bonds through thermolytic β-scission. **b**,**c**, Co/Mn/Br-mediated autoxidation of acetyl-protected lignin model compounds (part **b**) and acetyl-protected oligomers from poplar reductive catalytic fractionation oil[92] (part **c**). **d**, Comparison of acetyl-phenol and methyl-phenol protection for Mn/Zr-mediated autoxidation of monomers. **e**,**f**, Mn/Zr-mediated autoxidation of methyl-protected lignin model compounds (part **e**) and methyl-protected pine reductive catalytic fractionation-derived oligomers[93] (part **f**). Bonds represented in red highlight C–C cleavage points. Percent yields are reported as molar yields unless specifically stated as weight percent (wt%).

Brønsted acid sites to promote C–C cleavage

Acidic zeolites, featuring enhanced stability compared with sulfide catalysts, are versatile in that their acidity and average pore size can be tailored for various applications[107–109]. Brønsted acid sites within zeolites promote C–C bond cleavage through β-scission pathways, a process well-studied in alkane cracking[110–114]. In lignin depolymerization, these Brønsted acid sites activate lignin molecules by protonating functional groups, forming reactive carbenium ions as intermediates. These ions, stabilized by the acid sites, can undergo subsequent β-scission, breaking specific C–C bonds and yielding smaller lignin fragments[28,115].

Kong et al. used different types of zeolites to cleave methylene linkages in lignin model dimers, finding that commercial Hβ zeolite delivered the best catalytic performance owing to its high Brønsted acid site density and high surface area that afforded the exposure of more acid sites to the reactant[108]. Under optimal conditions, Hβ cleaved the methylene linkages in lignin model dimer compounds containing different alkyl groups through proton-induced scissions, leading to the formation of phenol with satisfactory yields (65–76 mol%) (Fig. 6c). Furthermore, by implementing a two-step strategy comprising initial C–O ether alcoholysis and subsequent C–C cleavage of dimers and oligomers, additional monomer yields of 7 to 10 wt% could be obtained from C–C bond cleavage (Fig. 6d).

By targeting the propyl side chain of phenolic monomers resulting from C–O bond cleavage, the complexity of product streams can be reduced. Sels and co-workers demonstrated that zeolites are adept at selectively cleaving the alkyl side chain of lignin-derived monomers to obtain phenol through steam-assisted dealkylation[116]. HZSM-5 was the most selective for dealkylating linear and branched propylphenols into phenol, an activity that was attributed to pore confinement that avoided transalkylation. This team also proposed an integrated biorefinery process to produce simultaneously 20 wt% of phenol and 9 wt% of propylene from wood lignin, thereby achieving high carbon efficiency. The tailor-made hierarchical ZSM-5 catalyst enables the selective dealkylation of biomass-derived crude alkylphenol streams, which can sustainably valorize birch wood into high-value end products[18] (Fig. 6e).

The sites of many solid acid catalysts are primarily located within micropores, which could pose challenges for large lignin-derived molecules in terms of mass transfer to access the active sites. Consequently, when using zeolitic catalysts for C–C cleavage, it is advisable to consider catalysts with larger pores or multiple levels of porosity that can potentially accommodate bulky lignin-derived molecules. Li et al. addressed this issue by using Cu catalysts supported on MFI nanosheets modified by Ce for the selective oxidative cleavage of C_α–C_β bonds in organosolv lignin[117]. The hierarchical Ce-Cu/MFI catalyst enabled the conversion of organosolv lignin under mild conditions at 150 °C for 24 hours, yielding 29 wt% of volatile products, including 18 wt% diethyl maleate, a result attributed to the cleavage of the benzene ring.

Bifunctional catalysts for promoting C–C cleavage

Although two-step C–O and C–C bond cleavage processes have proven successful in producing monomers in higher yields than processes involving C–O cleavage alone, the additional processing steps could increase process costs. An alternative strategy for achieving both C–O and C–C cleavage is to combine these functions within a single catalyst. Bifunctional metal-acid catalysts have emerged as pivotal players in facilitating various C–C bond cleavage chemistries[28,118–120]. The synergistic interplay between the metal and acid sites within the catalyst enhances the efficient breakdown of C–C bonds in lignin, ultimately leading to the production of valuable platform chemicals and aromatic compounds.

Dong et al. reported a one-pot catalytic method for monomer production from kraft, enzymatic, pine and birch lignins through hydrogenolytic C–O and C–C bond cleavage using a bifunctional $Ru/NbOPO_4$ catalyst[28] (Fig. 6f). Notably, this catalyst system produced benzene and C_6 cycloparaffins from biphenyl in model compound studies (representative of 5–5 cleavage in lignin). In terms of performance, up to 153 mol% of monocyclic hydrocarbons were produced relative to nitrobenzene oxidation yields (efficient only in C–O bond cleavage), a result attributed to C–C bond cleavage of lignin dimers and oligomers. The inclusion of Ru in the catalyst system provided hydrogenation activity, whereas the Brønsted acidic $NbOPO_4$ support played a crucial role in enhancing substrate adsorption and facilitating the cleavage of C–C bonds. The unique reactivity of $Ru/NbOPO_4$ compared with Ru/Nb_2O_5, Ru/TiO_2, Ru/ZrO_2, Ru/Al_2O_3 and Ru/HZSM-5 was attributed to the ability of $Ru/NbOPO_4$ to strongly adsorb the phenylcyclohexane intermediate and to its Brønsted acidic properties, which promote subsequent C–C scission[28,119]. The proposed reaction sequence included (1) adsorption of biphenyl on the catalyst surface, (2) protonation, (3) partial hydrogenation to phenylcyclohexane and (4) C–C bond cleavage followed by desorption of volatile products from the surface.

Meng and colleagues demonstrated the direct deconstruction of C_{sp2}–O and C_{sp2}–C_{sp3} bonds in phenylpropanol over a RuW/HY catalyst without saturation of the aromatic ring[121] (Fig. 6g,h). This resulted in the exclusive production of benzene, achieving a monomer yield of 19 wt% from lignin in the water system. The combination of Ru and W was necessary for the self-supported hydrogenolysis to remove the oxygen functional groups. The unique reactivity in this system is attributed to the higher electronegativity of Ru, which induces electron transfer from W to Ru. This strategy likely involves a stepwise protonated dehydroxylation, γ-methyl shift, and C_{sp2}–C_{sp3} bond β-scission pathway. Notably, with water as the reaction medium, this protocol can be readily scaled up to produce 8.5 g of benzene product from 50.0 g of lignin.

Luo et al. reported the scission of four common C–C bonds (β–5, β–β, 5–5 and β–1) in technical lignin using a bifunctional platinum mordenite (Pt/H-MOR) catalyst via a one-pot reductive catalytic approach[29]. This catalyst system achieved a monomer yield of 86 wt% by cleaving the 5–5 linkage in a biphenol model dimer at 260 °C and an H_2 pressure of 40 bar (Fig. 6i). Mechanistic investigations conducted utilizing various intermediates as feedstocks, along with density functional theory calculations, revealed that Pt/H-MOR cleaved aryl–aryl and alky–alkyl bonds via bifunctional catalysis;

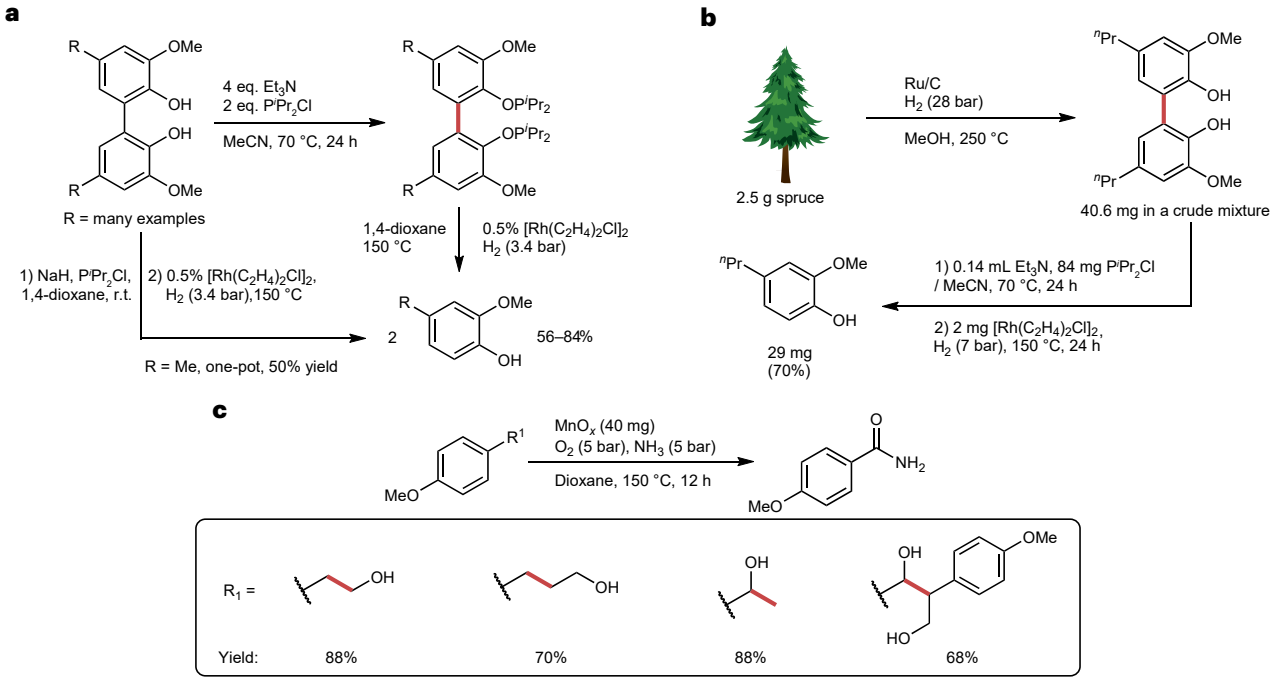

Fig. 5 | 5–5 cleavage and utilization of oxygen vacancies to promote lignin C–C cleavage. a,**b**, $[Rh(C_2H_4)_2Cl]_2$-mediated 5–5 cleavage of biphenyl lignin models to 4-alkylguaiacols (part **a**), and application of the $[Rh(C_2H_4)_2Cl]_2$ catalyst system on spruce wood reductive catalytic fractionation oil[99,100] (part **b**). **c**, MnO_x-mediated oxidation of lignin model compounds to produce amines and nitriles[104]. Bonds represented in red highlight C–C cleavage points. Percent yields are reported as molar yields unless specifically stated as weight percent (wt%).

Pt hydrogenates aryl moieties and introduces double bonds close to recalcitrant C–C bonds, and zeolitic Brønsted acid sites promote β-scission. Additionally, different dimer substrates linked by 5–5, β–1 and β–β bonds, featuring varied substituted functional groups, were evaluated at 280 °C, resulting in monocyclic hydrocarbon yields ranging from 83 to 98 wt% (Fig. 6i). This result validates reductive C–C cleavage by bifunctional Pt/H-MOR catalysts.

Upon the initial disruption of C–O bonds, Pt/H-MOR demonstrates the ability to depolymerize oligomers obtained by fractionation of hardwood at 300 °C, yielding a monomer yield up to 54.0 wt%[29]. The conversion of the lignin oil derived from birch wood improved the monomer yield to 76.9 wt%, nearly doubling the theoretical maximum monomer yield (Fig. 6j). The broader applicability of Pt/H-MOR was extended to the depolymerization of a range of lignins, resulting in substantial enhancement in monomer yields ranging between 6.0 and 16.8 wt% with kraft lignin, enzymatic-hydrolysis lignin, soda lignin and methanolysis lignin. The catalytic approach developed in this work enabled the selective breaking of various C–C linkages without pre-functionalization, representing a promising route for converting recalcitrant lignin waste into gasoline-range and jet-range cyclohexane and aromatics. Taken together, these works suggest the feasibility of metal-acid bifunctional catalysts in producing value-added products using lignin feedstocks.

The use of heterogeneous catalysts holds considerable promise for C–C bond cleavage to achieve elevated monomer yields in lignin depolymerization. Determining the ideal combination of metal and acidic supports is a key factor for selectively deconstructing C–C linkages. In addition, the pore geometry of the catalyst, the diffusion of reactants and products, and the steric hindrance of molecules all play crucial roles that must be considered for the efficient depolymerization of lignin.

Biological C–C bond cleavage in lignin

The recalcitrance of lignin is difficult to overcome even in biological systems, which has led to the evolution of a variety of enzymatic approaches, especially in white-rot fungi and in some selected bacteria, that contribute to lignin degradation in nature. The enzymes and catabolic pathways involved have been studied intensively, and they are summarized in multiple reviews[95,122–131]. According to the current knowledge, in nature, biological lignin degradation is typically considered to proceed via two primary pathways: (1) radical-mediated enzymatic oxidation (which is often non-selective) of lignocellulosic substrates, and (2) selective, enzyme-mediated catabolism of lower-molecular-weight lignin structures. These pathways are likely inter-connected, with the radical-mediated steps partially depolymerizing bulk lignin to smaller lignin oligomers and dimers, which are then fully catabolized through enzymatic degradation, representing a 'microbial sink' that depolymerizes lignin completely[132]. Throughout these processes, C–O and C–C bonds are cleaved through a variety of mechanisms.

Radical-mediated, non-selective enzymatic degradation of lignin

Initial depolymerization of native lignin is thought to be performed most efficiently by white-rot basidiomycetous fungi such as *Phanerochaete chrysosporium* through the extracellular action of a cocktail of oxidative, radical-mediated enzymes[133]. These include lignin peroxidases, manganese-dependent peroxidases and superoxide dismutases[134,135], versatile peroxidases, dye-decolourizing peroxidases[136], and laccases[127].

By contrast, although brown-rot fungi also perform some lignin degradation, they rely more on the secretion of reactive small molecules (that is, veratryl alcohol, phenolates, peptides, acids and so on). These molecules participate in oxidative deconstruction through the Fenton process (equation 1) with iron in the environment, acting as redox mediators to produce hydroxyl radicals that can attack lignin linkages[129].

$$Fe^{2+} + H_2O_2 \rightarrow Fe^{3+} + {}^{-}OH + {}^{\cdot}OH \quad (1)$$

More recently, researchers have discovered bacteria, such as *Amycolatopsis* and *Rhodococcus*, that also participate in lignin depolymerization through the secretion of similar oxidative enzymes as seen with white-rot fungi[127,129,137]. Although extensive work has been conducted to study the variety of organisms and enzymes involved in these radical-based degradation pathways, we posit that the actual depolymerization is best described as it was back in 1987 by Kirk and coworkers, as "enzymatic combustion"[138]. The oxidative enzymes and molecules generally perform a host of nonspecific oxidative cleavages of lignin and other molecules in the matrix (though there are suggestions of certain bacterial enzymes with more specificity for lignin[129]). A seminal discovery in 1983 described the observation of C_α–C_β cleavage of aryl–ether linkages in non-phenolic, methyl-protected lignin model compounds and spruce-derived lignin by a lignin peroxidase enzyme[139] (Fig. 7a). Subsequent studies have also proposed C_α–C_{aryl} bond cleavage pathways for certain peroxidases and dismutases[133,136,137]. Building on this evidence and additional studies[138–140], a general belief has been fostered in the literature that radical-mediated enzymes degrade lignin through these C–C cleavages of aryl-ether bonds, although there are limitations in the original work (non-phenolic and non-polymeric substrates). Other studies have contradicted this view, given that many radical-mediated enzymes (such as lignin peroxidase) actually polymerize phenolic lignin substrates under similar conditions[141]. Regardless, it is apparent that radical-mediated enzymatic lignin degradation is a complex process that is both non-selective and, at a minimum, targets β-aryl–ether linkages[129,132]. Given these difficulties in understanding and controlling radical-mediated lignin degradation, as well as the absence of concrete evidence that radical-mediated systems effectively cleave other common C–C linkages in lignin (such as β–1, β–5 and β–β)[122,127], we suggest that efforts to develop biological lignin deconstruction processes could focus on more selective, targeted degradation strategies — a prime example being the enzymatic catabolism of representative lignin dimers and monomers discussed below.

Enzymatic C–C bond cleavage for catabolism of lignin

Catabolism of low-molecular-weight lignin compounds is much better understood mechanistically than radical-mediated lignin degradation, at least in bacteria, and there is recent evidence for similar catabolic pathways in fungi as well[142]. The most well-studied systems — especially *Sphingobium* sp. SYK-6 and, more recently, *Novosphingobium aromaticivorans* DSM12444 — have helped elucidate multiple C–C bond cleavage steps, and, with *P. putida* KT2440 and *Rhodococcus jostii* RHA1, these microbes have increasingly been utilized in the bioconversion of lignin monomers and dimers. The most prevalent C–C cleavage mechanisms include decarboxylation, deformylation, oxidative cleavage, activated elimination, retro-aldol cleavage and catechol ring-opening (Fig. 7b). Here we focus on C–C cleavage reactions in aromatic dimers. For a more thorough overview of these reactions within the context of aromatic catabolic pathways by specific bacteria[134,136], we direct the reader towards more exhaustive reviews on the subject[122,125,127].

Most aryl-alkyl and aryl-ether lignin linkages, including β–O–4, β–5, β–1, 5–5 and β–β, are catabolized to either vanillate or syringate, depending on whether the monomer units are G-type or S-type, respectively. Many of these catabolic steps have been studied most exhaustively in SYK-6 (Fig. 7b), although C–C cleavage in the catabolism of β–β linkages has thus far been fully elucidated only in *Pseudomonas* SG-MS2 (refs. 143,144) (Supplementary Fig. 7). Both β–5 and β–1 linkages are degraded via a stilbene intermediate, requiring various decarboxylation and deformylation steps to reach the stilbene[145]. These steps can be complicated by the diastereomeric nature of β–1 dimers derived from ring-opened spirodienone linkages, requiring stereoselective enzymes. Recent work uncovered mechanisms and stereochemical requirements for the conversion of both *threo* and *erythro* β–1 dimers to stilbenes[146–148]. The stilbene intermediates then undergo C–C cleavage by the action of lignostilbene dioxygenases, which oxidatively break the bond to form two aldehyde products, including vanillin. The non-vanillin aldehyde product from β–5 cleavage still contains functionalities at the *para* and *ortho* positions that require further catabolism. An initial deformylation of the *ortho*-aldehyde represents one C–C cleavage step, followed by functionalization with coenzymeA (CoA) and H_2O to allow for a C–C cleaving elimination of AcCoA and the production of another molecule of vanillin. Although there is reported precedent for cleavage of the β–O–4 C_α–C_β bonds in some oxidative enzymatic treatments of model compounds by *P. chrysosporium*[138,139,149], the primary bacterial catabolism pathway instead begins with cleavage of the aryl ether C–O bond. Another activation of a carboxylic acid with CoA/H_2O again allows for a C–C bond-cleaving AcCoA elimination and the production of vanillate. Following production of vanillate and/or syringate from C–C cleavage of β–O–4, β–5 and β–1 linkages, the final catabolic steps involve ring opening of these aryl carboxylic acids to produce substrates such as pyruvate and oxaloacetate for the tricarboxylic acid cycle. These ring-opening reactions occur via either extradiol or intradiol cleavage of the respective catechols, depending on the enzymes involved.

In contrast to the alkyl and aryl ether linked structures, 5–5 lignin dimers initially require ring-opening C–C cleavage reactions for catabolism. Ring opening is preceded by an O-demethylation step that produces catechol substrates[150], which can then be enzymatically ring-opened. In the case of 5–5-linked lignin, this is an extradiol ring opening of one of the aryl rings, which is followed by oxidative cleavage of the resulting C_α–C_β bond. Decarboxylation of the remaining intact aryl ring produces vanillate for further catabolism[151], and the ring-opened fragment undergoes a retro-aldol C–C cleavage to produce pyruvate[152–154], which also enters the tricarboxylic acid cycle.

Uncovering the biological mechanisms has been the culmination of decades of research, but there are still many ongoing efforts to elucidate specific mechanistic details of degradation processes and to discover a wider range of involved enzymes and microorganisms. Additionally, applying biological methods to laboratory and industrial degradation is of particular interest; for example, despite the impressive efforts to uncover enzymatic activity on various lignin models and linkages, the direct application of enzymatic methods towards degrading bulk lignin substrates has not yet been explored extensively. There are a variety of challenges when translating fungal and bacterial degradation methods to industrial processes, although exploratory applications include fungal and/or bacterial pre-treatments of lignocellulose to remove lignin prior to pulping or biodiesel production[129]. Alternatively, many efforts have also been made to biologically valorize lignin-derived chemicals into

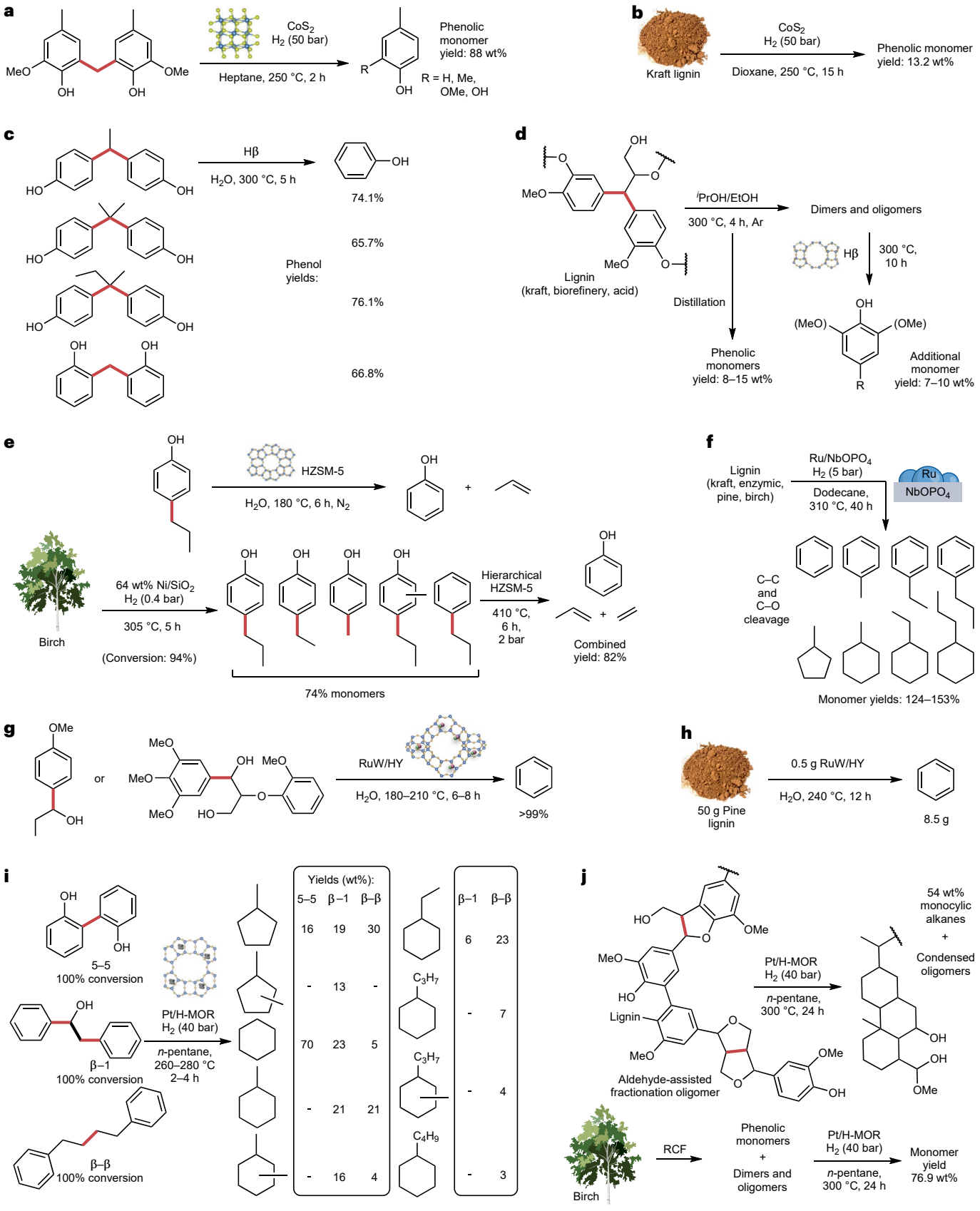
a
MeO
OMe
OH
OH
CoS2
H2 (50 bar)
Heptane, 250 °C, 2 h
R
OH
Phenolic monomer yield: 88 wt%
R = H, Me, OMe, OH
b
Kraft lignin
CoS2
H2 (50 bar)
Dioxane, 250 °C, 15 h
Phenolic monomer yield: 13.2 wt%
c
Hβ
H2O, 300 °C, 5 h
74.1%
65.7%
Phenol yields:
76.1%
66.8%
d
MeO
OH
Lignin (kraft, biorefinery, acid)
iPrOH/EtOH
300 °C, 4 h, Ar
Dimers and oligomers
Hβ
300 °C, 10 h
Distillation
Phenolic monomers yield: 8–15 wt%
(MeO)
(OMe)
R
Additional monomer yield: 7–10 wt%
e
HZSM-5
H2O, 180 °C, 6 h, N2
Birch
64 wt% Ni/SiO2
H2 (0.4 bar)
305 °C, 5 h
(Conversion: 94%)
Hierarchical HZSM-5
410 °C, 6 h, 2 bar
Combined yield: 82%
74% monomers
f
Lignin (kraft, enzymic, pine, birch)
Ru/NbOPO4
H2 (5 bar)
Dodecane, 310 °C, 40 h
Ru
NbOPO4
C–C and C–O cleavage
Monomer yields: 124–153%
g
OMe
OH
or
MeO
HO
RuW/HY
H2O, 180–210 °C, 6–8 h
>99%
h
50 g Pine lignin
0.5 g RuW/HY
H2O, 240 °C, 12 h
8.5 g
i
5–5
100% conversion
β–1
100% conversion
β–β
100% conversion
Pt/H-MOR
H2 (40 bar)
n-pentane, 260–280 °C 2–4 h
Yields (wt%):
5–5 β–1 β–β
16 19 30
- 13 -
70 23 5
- 21 21
- 16 4
C3H7
C3H7
C4H9
β–1 β–β
6 23
- 7
- 4
- 3
j
HO
OMe
MeO
HO
Lignin
MeO
OMe
OH
Aldehyde-assisted fractionation oligomer
Pt/H-MOR
H2 (40 bar)
n-pentane, 300 °C, 24 h
54 wt% monocylic alkanes
+
Condensed oligomers
OH
OH
OMe
Birch
RCF
Phenolic monomers
+
Dimers and oligomers
Pt/H-MOR
H2 (40 bar)
n-pentane, 300 °C, 24 h
Monomer yield 76.9 wt%

Fig. 6 | C–C bond cleavage with heterogeneous catalysis. a,**b**, Methylene linkage cleavage with a CoS_2 catalyst in a model compound (part **a**) and bulk lignin[106] (part **b**). **c**,**d**, Depolymerization of lignins with a solid acid catalyst[108]. **e**, Acid-catalysed cleavage of side chains in lignin-derived compounds to produce phenol with HZSM-5 zeolite[116]. **f**, One-pot catalytic production of aromatic monomers over a bifunctional $Ru/NbOPO_4$ catalyst[28]. **g**,**h**, $C_{aryl}–C_{\alpha}$ cleavage in model compounds over a bifunctional RuW/HY catalyst to yield benzene (part **g**) and application of this catalyst on bulk lignin[121] (part **h**). **i**,**j**, Reductive C–C cleavage of dimer substrates linked by 5–5, β–1 and β–β bonds over a bifunctional Pt/H-MOR catalyst (part **i**), and application of this cleavage method to technical lignins to produce monomers[29] (part **j**). Bonds represented in red highlight C–C cleavage points. Percent yields are reported as molar yields unless specifically stated as weight percent (wt%). Hβ, a proton-exchanged beta-type zeolite; HY, a high-silica (Si/Al>2) faujasite-type zeolite; HZSM-5 zeolite, a proton-exchanged Zeolite Socony Mobil-5; RCF, reductive catalytic fractionation; H-MOR, a proton-exchanged mordenite-type zeolite.

industrially useful products, particularly through the β-ketoadipate pathway[13,92,93,95,155–160].

Inspiration for future C–C bond cleavage efforts utilizing enzymes may be found in the work of Picart and coworkers, who applied enzyme systems for the biocatalytic depolymerization of C–O bonds in polymeric lignin substrates[161–165]. Their work systematically applied β-etherases for the cleavage of β-O-4 aryl-ether bonds, starting with simple model dimers and progressing to polymeric lignin substrates, including both OrganoCat[166] and synthetic lignins. We suggest that similar undertakings aimed at C–C cleavage are plausible; although many C–C cleavage enzymes have been uncovered in dimers and model compounds (vide supra), there is potential to apply these enzymes to polymeric lignin substrates, either on their own or in conjunction with C–O-cleaving β-etherases in multistep processes. Developing enzymatic systems that cleave both C–C and C–O bonds in polymeric substrates, such as OrganoCat[167], native-like[168] or ball-milled lignins, would represent a major step forward in biological lignin valorization efforts.

Conclusions and future directions

Here we have reviewed the various facets of lignin C–C bond cleavage with the goal of enhancing monomer yields beyond historical quantities primarily obtained through C–O bond cleavage. Given that lignin is a complex biopolymer with a diversity of linkages that are highly dependent on the feedstock and processing methods, the development of catalytic methods for high-yield C–C bond cleavage is challenging and requires a catalyst (or multiple catalysts) to process and tolerate a wide range of chemical functionalities. In any case, the research examples highlighted in this Review demonstrate multiple strategies that achieve C–C bond cleavage, including homogeneous methods, like those that directly activate O_2 and phenol groups, as well as heterogeneous, photocatalytic and biocatalytic approaches. We believe that these strategies, and others yet to be discovered, will play an integral role in improving monomer production from lignin, and we hope this summary will stimulate interest and encourage the development of new lignin C–C cleavage methods. As we look towards future breakthroughs in this field, we believe that there are

Glossary

β–O–4 linkage
The most abundant linkage in lignin; it comprises an aryl–ether C–O bond that links aryl propane units at the β-position of one unit and the 4-OH position of another.

Autoxidation
Refers to oxidations with oxygen, and it is characterized by a free radical chain process that is autocatalytic.

Bobbitt's salt
An oxoammonium compound derived from 4-acetamido-2,2,6,6-tetramethylpiperidine-N-oxyl and the tetrafuoroborate anion.

Enzymatic-hydrolysis lignin
A lignin-rich substrate obtained from the enzymatic hydrolysis of lignocellulose with cellulolytic enzymes.

Hβ zeolite
A proton-exchanged beta-type zeolite used widely in the petrochemical industry.

HY catalyst
A high-silica faujasite-type zeolite with Si/Al>2.

HZSM-5
A proton-exchanged Zeolite Socony Mobil-5, commonly abbreviated as ZSM-5.

Kraft lignin
A highly degraded lignin co-product of the kraft process utilized in the pulp and paper industry.

Kraft process
A widely used process that produces nearly pure holocellulose pulp. The process comprises heating biomass with sodium sulfide and sodium hydroxide, thereby dissolving lignin and facilitating its separation.

Lignin-first methods
Biomass fractionation methods that make use of active stabilization strategies to prevent lignin degradation through condensation reactivity.

Methanolysis lignin
Lignin obtained by methanolysis of biomass. Methanolysis cleaves primarily the ester linkages binding lignin and hemi-cellulose.

MFI
The zeolite framework type code of Zeolite Socony Mobil-5.

MOR
The zeolite framework type code of mordenite.

Organosolv lignin
A pulping technique that relies on an organic solvent to solubilize lignin, enabling its extraction and separation.

Reductive catalytic fractionation
(RCF). A lignin-first method that makes use of reduction with hydrogen to hydrogenolyse β–O–4 linkages and quench reactive unsaturated intermediates that could lead to condensation reactivity.

Soda lignin
Lignin obtained from soda pulping. The name of this pulping process comes from the use of caustic soda, or sodium hydroxide.

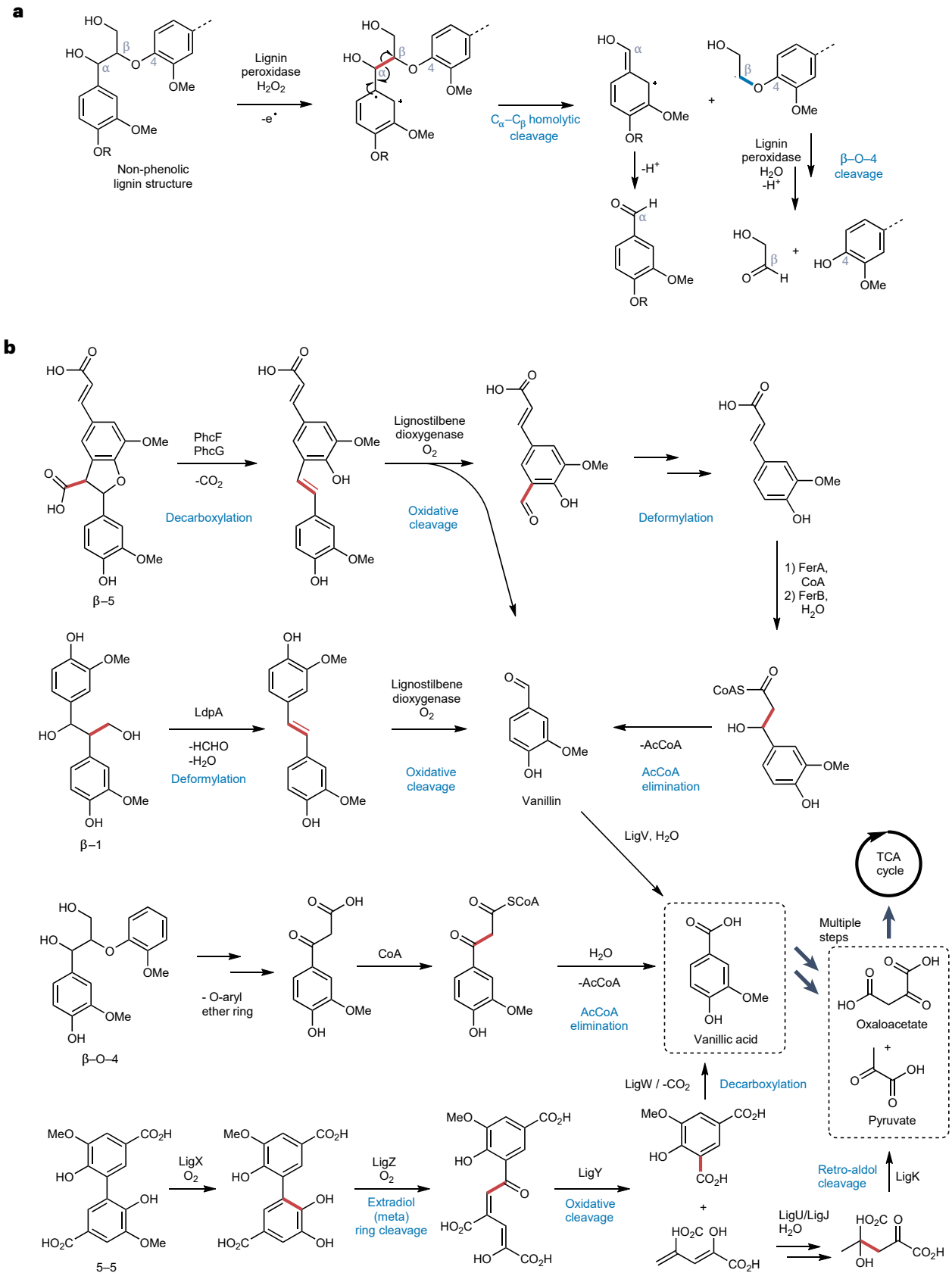
a
Non-phenolic lignin structure
Lignin peroxidase H_2O_2
-e•
C_α–C_β homolytic cleavage
-H+
Lignin peroxidase H_2O -H+
β–O–4 cleavage
b
PhcF PhcG
-CO_2
Decarboxylation
Lignostilbene dioxygenase O_2
Oxidative cleavage
Deformylation
1) FerA, CoA 2) FerB, H_2O
β–5
LdpA
-HCHO -H_2O
Deformylation
β–1
-AcCoA
AcCoA elimination
Vanillin
LigV, H_2O
- O-aryl ether ring
CoA
H_2O
-AcCoA
AcCoA elimination
Vanillic acid
β–O–4
TCA cycle
Multiple steps
Oxaloacetate
Pyruvate
LigW / -CO_2
Decarboxylation
LigX O_2
LigZ O_2
Extradiol (meta) ring cleavage
LigY
Oxidative cleavage
Retro-aldol cleavage
LigK
LigU/LigJ H_2O
5–5

Fig. 7 | Biological degradation of lignin. a, Selected example of radical-mediated enzymatic oxidation of a non-phenolic lignin substructure by a lignin peroxidase, highlighting the proposed C_α–C_β cleavage mechanism. Dashed lines represent additional, unspecified linkages to larger oligomers/polymers. Adapted from previous review[141]. **b**, Selected examples of C–C cleavage reactions in the bacterial catabolic funnelling of lignin dimers by *Sphingobium* sp. SYK-6 to vanillate. Simplified by only representing G-type (guaiacyl) lignin units, though full catabolism also funnels S-type (syringyl) units into syringate. Adapted from previous reviews[122,125]. Bonds represented in red highlight C–C cleavage points and bonds represented in blue highlight C–O cleavage. AcCoA, acetyl coenzyme A; TCA, tricarboxylic acid.

several outstanding areas of research worthy of pursuing, which we outline briefly below. Importantly, we also remark that it is first necessary to establish general guidelines for definitively studying and quantifying C–C bond cleavage in lignin to benchmark and compare catalytic approaches.

Guidelines for definitive C–C bond cleavage quantification in lignin

As evidenced in the C–C cleavage approaches discussed in this Review and in the vast lignin valorization literature not covered herein, research groups often take quite different approaches to experimentation, depending on the lignin source, catalytic methods, products quantification and reporting of yields. Some reports focus on only model compounds, from simple dimers and oligomers (non-phenolic and others) to more 'lignin-like' examples, whereas others incorporate polymeric lignin substrates from a variety of feedstocks and processing methods. This makes it difficult to rationally compare many catalytic approaches, an issue that is particularly present when researchers depolymerize lignin substrates that contain both C–O and C–C linkages. In these cases, when both bond types are targeted, it can be difficult to distinguish definitively between the two bond cleavage mechanisms and to accurately report C–C cleavage yields.

To definitively study C–C bond cleavage in lignin, investigations involving polymeric lignin substrates (in which the substrate is not strictly monomer-free and solely C–C linked) should include conducting control reactions to quantify the number of aryl ether (C–O) linkages first. To do this, a number of experimental approaches are appropriate, including thioacidolysis, direct functionalization through reductive cleavage and RCF, among others. Additionally, when possible, efforts should be made to separate monomers prior to catalysis (either through distillation[42,92,93], liquid/liquid chromatography[169] or other means). By first determining the quantity of aryl–ether linkages and monomer content in a lignin substrate, one can then normalize the measured catalytic yields with respect to those obtained from C–O cleavage alone with established methods. This is particularly relevant in the context of non-selective reactions that lead to deleterious product degradation, in which yields between C–C and C–O cleavage pathways are further confounded. Only then can one analyse the efficacy of particular catalyst systems relative to another.

Finally, a common occurrence throughout the C–C bond cleavage literature is the result that lignin model compound monomer yields are typically higher than monomer yields from polymeric lignin substrates (even for 'ideal' lignin substrates such as RCF oil). Generally, the simpler the lignin model/substrate, the higher the yield, and, because of the variety in model compounds and lignin substrates studied, this further confounds the comparison of catalytic systems. Accordingly, we suggest that, when possible, catalytic systems that show promise on model compounds should also be tested on lignin substrates to determine definitively their efficacy. By following these general guidelines, we believe that future C–C cleavage research will be more effectively reported and its results will be more comparable, leading to a faster identification of the most promising catalytic pathways.

Areas for future exploration

Although the number of strategies for C–C cleavage is increasing, the field would benefit from improved fractionation methods. New types of lignin substrates with divergent functional groups would further broaden the chemistry available for subsequent C–C cleavage. For example, C–C cleavage of RCF lignin oils is hampered by the saturated propyl side chain, which is difficult to activate without highly reactive reagents, whose use can lead to over-reactivity and decreased monomer yields. Therefore, we advocate for the development of new lignin isolation methods that produce lignins functionalized for subsequent C–C cleavage.

Another avenue for exploration is to apply flow chemistry to overcome selectivity issues in batch reactors, which should lead to greater product yields. Additionally, efforts should be directed towards producing single products. The heterogeneity of lignin-derived aromatics can yield complex product mixtures upon deconstruction, complicating valorization. C–C cleavage has the potential to simplify these streams by eliminating variability through cleavage of the propyl side chain.

Finally, photocatalysis provides a number of potential advantages in the valorization of lignin, particularly given that it provides a delignification process that can utilize a sustainable energy source such as visible light (see Supplementary Information for specific examples). Additionally, photocatalysis can often be conducted under mild reaction conditions or with non-toxic reagents, and it also has the potential to drive otherwise forbidden reactions[170]. However, to date, the majority of lignin-related photocatalysis studies have focused on aryl–ether bonds in model compounds[171]. Although promising conversions and yields have been reported for these linkages (such as β–O–4), and the said conversions often proceed through a C–C cleavage pathway, the overall substrate scopes are lacking in terms of model compounds with non-ethereal linkages (such as β–1, β–5, β–β and 5–5). Some recent studies have started to investigate some of these other linkages in more depth[172], but the majority of β–O–4 and β–1 model compounds studied thus far are non-phenolic and/or require an α-OH/α-ketone group. That means that many of these models are not particularly representative of the linkages in a large percentage of polymeric lignin substrates, and we believe there is substantial space for increased efforts in this area in terms of moving towards more 'lignin-like' models. Indeed, uncovering the effectiveness of photocatalysis for cleaving C–C-based linkages in these more complex substrates will be important to determine the true potential of photocatalysis in the context of overall lignin valorization efforts.

Published online: 04 October 2024

References

1. Katahira, R., Elder, T. J. & Beckham, G. T. in *Lignin Valorization: Emerging Approaches* (ed. Beckham, G. T.) Ch. 1 (The Royal Society of Chemistry, 2018).
2. del Río, J. C. et al. Lignin monomers from beyond the canonical monolignol biosynthetic pathway: another brick in the wall. *ACS Sustain. Chem. Eng.* **8**, 4997–5012 (2020).
3. del Río J. C. et al. in *Recent Advances in Polyphenol Research* Vol. 7 (eds Dreher Reed, J. et al.) Ch. 7 (Wiley, 2021).

4. Campbell, M. M. & Sederoff, R. R. Variation in lignin content and composition (mechanisms of control and implications for the genetic improvement of plants). *Plant Physiol.* **110**, 3–13 (1996).
5. Cabane, M., Afif, D. & Hawkins S. in *Advances in Botanical Research* Vol. 61 (eds Jouanin, L. & Lapierre, C.) Ch. 7 (Academic Press, 2012).
6. Aro, T. & Pedram, F. Production and application of lignosulfonates and sulfonated lignin. *ChemSusChem* **10**, 1861–1877 (2017).
7. Corona, A. et al. Life cycle assessment of adipic acid production from lignin. *Green Chem.* **20**, 3857–3866 (2018).
8. Huang, K., Fasahati, P. & Maravelias, C. T. System-level analysis of lignin valorization in lignocellulosic biorefineries. *iScience* **23**, 100751 (2020).
9. Davis R., et al. *Process Design and Economics for the Conversion of Lignocellulosic Biomass to Hydrocarbons: Dilute-acid Prehydrolysis and Enzymatic Hydrolysis Deconstruction of Biomass to Sugars and Biological Conversion of Sugars to Hydrocarbons*. Technical Report NREL/TP-5100-60223 (National Renewable Energy Laboratory, 2013).
10. Zakzeski, J., Bruijnincx, P. C., Jongerius, A. L. & Weckhuysen, B. M. The catalytic valorization of lignin for the production of renewable chemicals. *Chem. Rev.* **110**, 3552–3599 (2010).
11. Li, C., Zhao, X., Wang, A., Huber, G. W. & Zhang, T. Catalytic transformation of lignin for the production of chemicals and fuels. *Chem. Rev.* **115**, 11559–11624 (2015).
12. Rinaldi, R. et al. Paving the way for lignin valorisation: recent advances in bioengineering, biorefining and catalysis. *Angew. Chem. Int. Ed.* **55**, 8164–8215 (2016).
13. Schutyser, W. et al. Chemicals from lignin: an interplay of lignocellulose fractionation, depolymerisation, and upgrading. *Chem. Soc. Rev.* **47**, 852–908 (2018).
14. Sun, Z., Fridrich, B., de Santi, A., Elangovan, S. & Barta, K. Bright side of lignin depolymerization: toward new platform chemicals. *Chem. Rev.* **118**, 614–678 (2018).
15. Wong, S. S., Shu, R., Zhang, J., Liu, H. & Yan, N. Downstream processing of lignin derived feedstock into end products. *Chem. Soc. Rev.* **49**, 5510–5560 (2020).
16. Questell-Santiago, Y. M., Galkin, M. V., Barta, K. & Luterbacher, J. S. Stabilization strategies in biomass depolymerization using chemical functionalization. *Nat. Rev. Chem.* **4**, 311–330 (2020).
17. Renders, T., Van den Bosch, S., Koelewijn, S. F., Schutyser, W. & Sels, B. Lignin-first biomass fractionation: the advent of active stabilisation strategies. *Energy Environ. Sci.* **10**, 1551–1557 (2017).
18. Liao, Y. et al. A sustainable wood biorefinery for low-carbon food-print chemicals production. *Science* **367**, 1385–1390 (2020).
19. Cui, Y., Goes, S. L. & Stahl, S. S. Sequential oxidation-depolymerization strategies for lignin conversion to low molecular weight aromatic chemicals. *Adv. Inorg. Chem.* **77**, 99–136 (2021).
20. Rahimi, A., Ulbrich, A., Coon, J. J. & Stahl, S. S. Formic-acid-induced depolymerization of oxidized lignin to aromatics. *Nature* **515**, 249–252 (2014).
21. Deuss, P. J. et al. Aromatic monomers by *in situ* conversion of reactive intermediates in the acid-catalyzed depolymerization of lignin. *J. Am. Chem. Soc.* **137**, 7456–7467 (2015).
22. Shuai, L. et al. Formaldehyde stabilization facilitates lignin monomer production during biomass depolymerization. *Science* **354**, 329–333 (2016).
23. Boerjan, W., Ralph, J. & Baucher, M. Lignin biosynthesis. *Annu. Rev. Plant Biol.* **54**, 519–546 (2003).
24. Guadix-Montero, S. & Sankar, M. Review on catalytic cleavage of C–C inter-unit linkages in lignin model compounds: towards lignin depolymerisation. *Top. Catal.* **61**, 183–198 (2018).
25. Hanson, S. K. & Baker, R. T. Knocking on wood: base metal complexes as catalysts for selective oxidation of lignin models and extracts. *Acc. Chem. Res.* **48**, 2037–2048 (2015).
26. Liu, H., Li, H., Luo, N. & Wang, F. Visible-light-induced oxidative lignin C–C bond cleavage to aldehydes using vanadium catalysts. *ACS Catal.* **10**, 632–643 (2020).
27. Zhang, Q. et al. Mechanistic insights into the photocatalytic valorization of lignin models via C–O/C–C cleavage or C–C/C–N coupling. *Chem Catalysis* **3**, 100470 (2023).
28. Dong, L. et al. Breaking the limit of lignin monomer production via cleavage of interunit carbon–carbon linkages. *Chem* **5**, 1521–1536 (2019).
29. Luo, Z. et al. Carbon–carbon bond cleavage for a lignin refinery. *Nat. Chem. Eng.* **1**, 61–72 (2024).
30. Lutz, M. D. & Morandi, B. Metal-catalyzed carbon–carbon bond cleavage of unstrained alcohols. *Chem. Rev.* **121**, 300–326 (2020).
31. Lu, H., Yu, T.-Y., Xu, P.-F. & Wei, H. Selective decarbonylation via transition-metal-catalyzed carbon–carbon bond cleavage. *Chem. Rev.* **121**, 365–411 (2020).
32. Jun, C.-H. Transition metal-catalyzed carbon–carbon bond activation. *Chem. Soc. Rev.* **33**, 610–618 (2004).
33. Liu, H., Feng, M. & Jiang, X. Unstrained carbon–carbon bond cleavage. *Chem. Asian J.* **9**, 3360–3389 (2014).
34. McDonald, T. R., Mills, L. R., West, M. S. & Rousseaux, S. A. Selective carbon–carbon bond cleavage of cyclopropanols. *Chem. Rev.* **121**, 3–79 (2020).
35. Chen, F., Wang, T. & Jiao, N. Recent advances in transition-metal-catalyzed functionalization of unstrained carbon–carbon bonds. *Chem. Rev.* **114**, 8613–8661 (2014).
36. Amadio, E., Di Lorenzo, R., Zonta, C. & Licini, G. Vanadium catalyzed aerobic carbon–carbon cleavage. *Coord. Chem. Rev.* **301**, 147–162 (2015).
37. Allpress, C. J. & Berreau, L. M. Oxidative aliphatic carbon–carbon bond cleavage reactions. *Coord. Chem. Rev.* **257**, 3005–3029 (2013).
38. Chen, H. et al. Mechanism insight into photocatalytic conversion of lignin for valuable chemicals and fuels production: a state-of-the-art review. *Renew. Sustain. Energy Rev.* **147**, 111217 (2021).
39. Wong, D. W. Structure and action mechanism of ligninolytic enzymes. *Appl. Biochem. Biotechnol.* **157**, 174–209 (2009).
40. Gharehkhani, S., Zhang, Y. & Fatehi, P. Lignin-derived platform molecules through TEMPO catalytic oxidation strategies. *Prog. Energy Combust. Sci.* **72**, 59–89 (2019).
41. Whetten, R. & Sederoff, R. Lignin biosynthesis. *Plant Cell* **7**, 1001–1013 (1995).
42. Subbotina, E. et al. Oxidative cleavage of C–C bonds in lignin. *Nat. Chem.* **13**, 1118–1125 (2021).
43. Renders, T., Van den Bossche, G., Vangeel, T., Van Aelst, K. & Sels, B. Reductive catalytic fractionation: state of the art of the *lignin-first* biorefinery. *Curr. Opin. Biotechnol.* **56**, 193–201 (2019).
44. Bartling, A. W. et al. Techno-economic analysis and life cycle assessment of a biorefinery utilizing reductive catalytic fractionation. *Energy Environ. Sci.* **14**, 4147–4168 (2021).
45. Tanahashi, M., Takeuchi, H. & Higuchi, T. Dehydrogenative polymerization of 3,5-disubstituted p-coumaryl alcohols. *Wood Res. Bull. Wood Res. Inst. Kyoto Univ.* **61**, 44–53 (1976).
46. Sasaki, S., Nishida, T., Tsutsumi, Y. & Kondo, R. Lignin dehydrogenative polymerization mechanism: a poplar cell wall peroxidase directly oxidizes polymer lignin and produces in vitro dehydrogenative polymer rich in β-O-4 linkage. *FEBS Lett.* **562**, 197–201 (2004).
47. Liu, C.-J. Deciphering the enigma of lignification: precursor transport, oxidation, and the topochemistry of lignin assembly. *Mol. Plant* **5**, 304–317 (2012).
48. Syrjänen, K. & Brunow, G. Regioselectivity in lignin biosynthesis. The influence of dimerization and cross-coupling. *J. Chem. Soc. Perkin Trans. 1* **2000**, 183–187 (2000).
49. Önnerud, H., Zhang, L., Gellerstedt, G. R. & Henriksson, G. Polymerization of monolignols by redox shuttle–mediated enzymatic oxidation: a new model in lignin biosynthesis I. *Plant Cell* **14**, 1953–1962 (2002).
50. Gani, T. Z. et al. Computational evidence for kinetically controlled radical coupling during lignification. *ACS Sustain. Chem. Eng.* **7**, 13270–13277 (2019).
51. van Parijs, F. R., Morreel, K., Ralph, J., Boerjan, W. & Merks, R. M. Modeling lignin polymerization. I. simulation model of dehydrogenation polymers. *Plant Physiol.* **153**, 1332–1344 (2010).
52. Thi, H. D. et al. Identification and quantification of lignin monomers and oligomers from reductive catalytic fractionation of pine wood with GC× GC–FID/MS. *Green Chem.* **24**, 191–206 (2022).
53. Stewart, J. J., Akiyama, T., Chapple, C., Ralph, J. & Mansfield, S. D. The effects on lignin structure of overexpression of ferulate 5-hydroxylase in hybrid poplar. *Plant Physiol.* **150**, 621–635 (2009).
54. Anderson, E. M. et al. Differences in S/G ratio in natural poplar variants do not predict catalytic depolymerization monomer yields. *Nat. Commun.* **10**, 2033 (2019).
55. Dao Thi, H. et al. Identification and quantification of lignin monomers and oligomers from reductive catalytic fractionation of pine wood with GC × GC – FID/MS. *Green Chem.* **24**, 191–206 (2022).
56. Abu-Omar, M. M. et al. Guidelines for performing lignin-first biorefining. *Energy Environ. Sci.* **14**, 262–292 (2021).
57. Gargulak, J. D., Lebo, S. E. & McNally, T. J. in *Kirk-Othmer Encyclopedia of Chemical Technology* 1–26 (Wiley, 2000).
58. Patt, R. et al. in *Ullmann's Encyclopedia of Industrial Chemistry* (Wiley-VCH, 2000); https://doi.org/10.1002/14356007.a18_545.
59. Crestini, C., Lange, H., Sette, M. & Argyropoulos, D. S. On the structure of softwood kraft lignin. *Green Chem.* **19**, 4104–4121 (2017).
60. Giummarella, N., Lindén, P. A., Areskogh, D. & Lawoko, M. Fractional profiling of kraft lignin structure: unravelling insights on lignin reaction mechanisms. *ACS Sustain. Chem. Eng.* **8**, 1112–1120 (2019).
61. Lancefield, C. S., Wienk, H. L. J., Boelens, R., Weckhuysen, B. M. & Bruijnincx, P. C. A. Identification of a diagnostic structural motif reveals a new reaction intermediate and condensation pathway in kraft lignin formation. *Chem. Sci.* **9**, 6348–6360 (2018).
62. Bolzacchini, E. et al. Oxidation of propenoidic phenols catalysed by N, N-ethylenebis(salicylideneiminato)cobalt(II)[Cosalen]: reactivity and spectroscopic studies. *J. Mol. Catal. A Chem.* **112**, 347–351 (1996).
63. Drago, R., Corden, B. & Barnes, C. Novel cobalt(II)-catalyzed oxidative cleavage of a carbon-carbon double bond. *J. Am. Chem. Soc.* **108**, 2453–2454 (1986).
64. Zombeck, A., Drago, R. S., Corden, B. B. & Gaul, J. H. Activation of molecular oxygen. Kinetic studies of the oxidation of hindered phenols with cobalt-dioxygen complexes. *J. Am. Chem. Soc.* **103**, 7580–7585 (1981).
65. Biannic, B., Bozell, J. J. & Elder, T. Steric effects in the design of Co-Schiff base complexes for the catalytic oxidation of lignin models to *para*-benzoquinones. *Green Chem.* **16**, 3635–3642 (2014).
66. Canevali, C. et al. Oxidative degradation of monomeric and dimeric phenylpropanoids: reactivity and mechanistic investigation. *J. Chem. Soc. Dalton Trans.* **15**, 3007–3014 (2002).
67. Biannic, B. & Bozell, J. J. Efficient cobalt-catalyzed oxidative conversion of lignin models to benzoquinones. *Org. Lett.* **15**, 2730–2733 (2013).
68. Bozell, J. J., Hames, B. R. & Dimmel, D. R. Cobalt-Schiff base complex catalyzed oxidation of para-substituted phenolics. Preparation of benzoquinones. *J. Org. Chem.* **60**, 2398–2404 (1995).
69. Bolzacchini, E. et al. Spectromagnetic investigation of the active species in the oxidation of propenoidic phenols catalysed by [*N,N'*-bis(salicylidene)ethane-1,2-diaminato] cobalt(II). *J. Chem. Soc. Dalton Trans.* **1997**, 4695–4700 (1997).

70. Cooper, C. J. et al. Co(salen)-catalyzed oxidation of lignin models to form benzoquinones and benzaldehydes: a computational and experimental study. *ACS Sustain. Chem. Eng.* **8**, 7225–7234 (2020).
71. Floriani, C. & Calderazzo, F. Oxygen adducts of Schiff's base complexes of cobalt prepared in solution. *J. Chem. Soc. A Inorg. Phys. Theoret.* **1969**, 946–953 (1969).
72. Sedai, B. et al. Aerobic oxidation of β-1 lignin model compounds with copper and oxovanadium catalysts. *ACS Catal.* **3**, 3111–3122 (2013).
73. Wigington, B. N. et al. A biomimetic pathway for vanadium-catalyzed aerobic oxidation of alcohols: evidence for a base-assisted dehydrogenation mechanism. *Chem. Eur. J.* **18**, 14981–14988 (2012).
74. Tarabanko, V., Fomova, N., Kuznetsov, B., Ivanchenko, N. & Kudryashev, A. On the mechanism of vanillin formation in the catalytic oxidation of lignin with oxygen. *React. Kinet. Catal. Lett.* **55**, 161–170 (1995).
75. Rahimi, A., Azarpira, A., Kim, H., Ralph, J. & Stahl, S. S. Chemoselective metal-free aerobic alcohol oxidation in lignin. *J. Am. Chem. Soc.* **135**, 6415–6418 (2013).
76. Cho, D. W. et al. Nature and kinetic analysis of carbon–carbon bond fragmentation reactions of cation radicals derived from SET-oxidation of lignin model compounds. *J. Org. Chem.* **75**, 6549–6562 (2010).
77. Forrester, I. T., Grabski, A. C., Burgess, R. R. & Leatham, G. F. Manganese, Mn-dependent peroxidases, and the biodegradation of lignin. *Biochem. Biophys. Res. Commun.* **157**, 992–999 (1988).
78. Hoover, J. M., Ryland, B. L. & Stahl, S. S. Mechanism of copper(I)/TEMPO-catalyzed aerobic alcohol oxidation. *J. Am. Chem. Soc.* **135**, 2357–2367 (2013).
79. Hoover, J. M., Ryland, B. L. & Stahl, S. S. Copper/TEMPO-catalyzed aerobic alcohol oxidation: mechanistic assessment of different catalyst systems. *ACS Catal.* **3**, 2599–2605 (2013).
80. McCann, S. D. & Stahl, S. S. Copper-catalyzed aerobic oxidations of organic molecules: pathways for two-electron oxidation with a four-electron oxidant and a one-electron redox-active catalyst. *Acc. Chem. Res.* **48**, 1756–1766 (2015).
81. Kinoshita, K. On the mechanism of oxidation by cuprous chloride, pyridine and air. I. The properties of the reaction. *Bull. Chem. Soc. Jpn.* **32**, 777–780 (1959).
82. Rogic, M. M. & Demmin, T. R. Cleavage of carbon-carbon bonds. Copper(II)-induced oxygenolysis of o-benzoquinones, catechols, and phenols. On the question of nonenzymic oxidation of aromatics and activation of molecular oxygen. *J. Am. Chem. Soc.* **100**, 5472–5487 (1978).
83. Tang, C. & Jiao, N. Copper-catalyzed aerobic oxidative C–C bond cleavage for C–N bond formation: from ketones to amides. *Angew. Chem.* **126**, 6646–6650 (2014).
84. Huang, X. et al. From ketones to esters by a Cu-catalyzed highly selective C (CO)–C (alkyl) bond cleavage: aerobic oxidation and oxygenation with air. *J. Am. Chem. Soc.* **136**, 14858–14865 (2014).
85. Qiu, X. et al. Cleaving arene rings for acyclic alkenylnitrile synthesis. *Nature* **597**, 64–69 (2021).
86. Zhou, Z.-z, Liu, M. & Li, C.-J. Selective copper–N-heterocyclic carbene (copper-NHC)-catalyzed aerobic cleavage of β-1 lignin models to aldehydes. *ACS Catal.* **7**, 3344–3348 (2017).
87. Kim, S. A., Kim, S. E., Kim, Y. K. & Jang, H.-Y. Copper-catalyzed oxidative cleavage of the C–C bonds of β-alkoxy alcohols and β-1 compounds. *ACS Omega* **5**, 31684–31691 (2020).
88. Hu, Y. et al. Mild selective oxidative cleavage of lignin C–C bonds over a copper catalyst in water. *Green Chem.* **23**, 7030–7040 (2021).
89. Partenheimer, W. The aerobic oxidative cleavage of lignin to produce hydroxyaromatic benzaldehydes and carboxylic acids via metal/bromide catalysts in acetic acid/water mixtures. *Adv. Synth. Catal.* **351**, 456–466 (2009).
90. Partenheimer, W. The unusual characteristics of the aerobic oxidation of 3,4-dimethoxytoluene with metal/bromide catalysts. *Adv. Synth. Catal.* **346**, 1495–1500 (2004).
91. Clatworthy, E. B. et al. Investigating homogeneous Co/Br^-/H_2O_2 catalysed oxidation of lignin model compounds in acetic acid. *Catal. Sci. Technol.* **9**, 384–397 (2019).
92. Gu, N. X. et al. Autoxidation catalysis for carbon–carbon bond cleavage in lignin. *ACS Cent. Sci.* **9**, 2277–2285 (2023).
93. Palumbo, C. T. et al. Catalytic carbon–carbon bond cleavage in lignin via manganese–zirconium-mediated autoxidation. *Nat. Commun.* **15**, 862 (2024).
94. Erickson, E. et al. Critical enzyme reactions in aromatic catabolism for microbial lignin conversion. *Nat. Catal.* **5**, 86–98 (2022).
95. Beckham, G. T., Johnson, C. W., Karp, E. M., Salvachúa, D. & Vardon, D. R. Opportunities and challenges in biological lignin valorization. *Curr. Opin. Biotechnol.* **42**, 40–53 (2016).
96. Becker, J. & Wittmann, C. A field of dreams: lignin valorization into chemicals, materials, fuels, and health-care products. *Biotechnol. Adv.* **37**, 107360 (2019).
97. Kim, S. et al. Computational study of bond dissociation enthalpies for a large range of native and modified lignins. *J. Phys. Chem. Lett.* **2**, 2846–2852 (2011).
98. Parthasarathi, R., Romero, R. A., Redondo, A. & Gnanakaran, S. Theoretical study of the remarkably diverse linkages in lignin. *J. Phys. Chem. Lett.* **2**, 2660–2666 (2011).
99. Zhu, J., Wang, J. & Dong, G. Catalytic activation of unstrained C (aryl)–C (aryl) bonds in 2, 2-biphenols. *Nat. Chem.* **11**, 45–51 (2019).
100. Zhu, J., Chen, P.-H., Lu, G., Liu, P. & Dong, G. Ruthenium-catalyzed reductive cleavage of unstrained aryl–aryl bonds: reaction development and mechanistic study. *J. Am. Chem. Soc.* **141**, 18630–18640 (2019).
101. Oregui-Bengoechea, M. et al. Heterogeneous catalyzed thermochemical conversion of lignin model compounds: an overview. *Top. Curr. Chem.* **377**, 36 (2019).
102. Gale, M., Cai, C. M. & Gilliard-Abdul-Aziz, K. L. Heterogeneous catalyst design principles for the conversion of lignin into high-value commodity fuels and chemicals. *ChemSusChem* **13**, 1947–1966 (2020).
103. Awan I. Z., et al. F. in *Studies in Surface Science and Catalysis*, Vol. 178 (eds Albonetti, S. et al.) Ch. 13 (Elsevier, 2019).
104. He, P. et al. Heterogeneous manganese-oxide-catalyzed successive cleavage and functionalization of alcohols to access amides and nitriles. *Chem* **8**, 1906–1927 (2022).
105. Wei, X. Y., Ogata, E., Zong, Z. M. & Niki, E. Effects of hydrogen pressure, sulfur, and iron sulfide (FeS2) on diphenylmethane hydrocracking. *Energy Fuels* **6**, 868–869 (1992).
106. Shuai, L. et al. Selective C–C bond cleavage of methylene-linked lignin models and kraft lignin. *ACS Catal.* **8**, 6507–6512 (2018).
107. Deepa, A. K. & Dhepe, P. L. Lignin depolymerization into aromatic monomers over solid acid catalysts. *ACS Catal.* **5**, 365–379 (2015).
108. Kong, X., Liu, C., Fan, Y., Li, M. & Xiao, R. Depolymerization of methylene linkage in condensed lignin with commercial zeolite in water. *ACS Catal.* **13**, 10048–10055 (2023).
109. Kong, X., Liu, C., Zeng, H., Fan, Y. & Zhang, H. Xiao R. Selective cleavage of methylene linkage in kraft lignin over commercial zeolite in isopropanol. *ChemSusChem* **17**, e202300996 (2024).
110. Corma, A., Planelles, J., Sánchez-Marín, J. & Tomás, F. The role of different types of acid site in the cracking of alkanes on zeolite catalysts. *J. Catal.* **93**, 30–37 (1985).
111. Li, Q. & East, A. L. Catalyzed β scission of a carbenium ion — mechanistic differences from varying catalyst basicity. *Can. J. Chem.* **83**, 1146–1157 (2005).
112. Weitkamp, J. Catalytic hydrocracking—mechanisms and versatility of the process. *ChemCatChem* **4**, 292–306 (2012).
113. Noh, G., Zones, S. I. & Iglesia, E. Consequences of acid strength and diffusional constraints for alkane isomerization and β-scission turnover rates and selectivities on bifunctional metal-acid catalysts. *J. Phys. Chem. C* **122**, 25475–25497 (2018).
114. Kotrel, S., Knözinger, H. & Gates, B. C. The Haag–Dessau mechanism of protolytic cracking of alkanes. *Microporous Mesoporous Mater.* **35-36**, 11–20 (2000).
115. Yan, J. et al. Selective valorization of lignin to phenol by direct transformation of C_{sp2}–C_{sp3} and C–O bonds. *Sci. Adv.* **6**, eabd1951 (2020).
116. Liao, Y. et al. Propylphenol to phenol and propylene over acidic zeolites: role of shape selectivity and presence of steam. *ACS Catal.* **8**, 7861–7878 (2018).
117. Li, L. et al. Selective aerobic oxidative cleavage of lignin C–C bonds over novel hierarchical Ce-Cu/MFI nanosheets. *Appl. Catal. B* **279**, 119343 (2020).
118. Zhang, W. et al. Hydrodeoxygenation of lignin-derived phenolic monomers and dimers to alkane fuels over bifunctional zeolite-supported metal catalysts. *ACS Sustain. Chem. Eng.* **2**, 683–691 (2014).
119. Dong, L. et al. Mechanisms of $C_{aromatic}$–C bonds cleavage in lignin over NbO_x-supported Ru catalyst. *J. Catal.* **394**, 94–103 (2021).
120. Fang, Q. et al. Low temperature catalytic conversion of oligomers derived from lignin in pubescens on Pd/$NbOPO_4$. *Appl. Catal. B* **263**, 118325 (2020).
121. Meng, Q. et al. Sustainable production of benzene from lignin. *Nat. Commun.* **12**, 4534 (2021).
122. Bugg, T. D., Ahmad, M., Hardiman, E. M. & Rahmanpour, R. Pathways for degradation of lignin in bacteria and fungi. *Nat. Prod. Rep.* **28**, 1883–1896 (2011).
123. Cragg, S. M. et al. Lignocellulose degradation mechanisms across the Tree of Life. *Curr. Opin. Chem. Biol.* **29**, 108–119 (2015).
124. Asina, F. N. U., Brzonova, I., Kozliak, E., Kubátová, A. & Ji, Y. Microbial treatment of industrial lignin: successes, problems and challenges. *Renew. Sustain. Energy Rev.* **77**, 1179–1205 (2017).
125. Kamimura, N. et al. Bacterial catabolism of lignin-derived aromatics: new findings in a recent decade: update on bacterial lignin catabolism. *Environ. Microbiol. Rep.* **9**, 679–705 (2017).
126. Brink, D. P., Ravi, K., Lidén, G. & Gorwa-Grauslund, M. F. Mapping the diversity of microbial lignin catabolism: experiences from the eLignin database. *Appl. Microbiol. Biotechnol.* **103**, 3979–4002 (2019).
127. Kamimura, N., Sakamoto, S., Mitsuda, N., Masai, E. & Kajita, S. Advances in microbial lignin degradation and its applications. *Curr. Opin. Biotechnol.* **56**, 179–186 (2019).
128. Li, X. & Zheng, Y. Biotransformation of lignin: mechanisms, applications and future work. *Biotechnol. Prog.* **36**, e2922 (2020).
129. Atiwesh, G., Parrish, C. C., Banoub, J. & Le, T. T. Lignin degradation by microorganisms: a review. *Biotechnol. Prog.* **38**, e3226 (2022).
130. Grgas, D. et al. The bacterial degradation of lignin—a Review. *Water* **15**, 1272 (2023).
131. Bugg, T. D. H. The chemical logic of enzymatic lignin degradation. *Chem. Commun.* **60**, 804–814 (2024).
132. Salvachúa, D. et al. Lignin depolymerization by fungal secretomes and a microbial sink. *Green Chem.* **18**, 6046–6062 (2016).
133. Tuor, U., Wariishi, H., Schoemaker, H. E. & Gold, M. H. Oxidation of phenolic arylglycerol β-aryl ether lignin model compounds by manganese peroxidase from *Phanerochaete chrysosporium*: oxidative cleavage of an. α-carbonyl model compound. *Biochemistry* **31**, 4986–4995 (1992).
134. Rashid, G. M. et al. Identification of manganese superoxide dismutase from *Sphingobacterium sp*. T2 as a novel bacterial enzyme for lignin oxidation. *ACS Chem. Biol.* **10**, 2286–2294 (2015).
135. Rashid, G. M. et al. *Sphingobacterium sp*. T2 manganese superoxide dismutase catalyzes the oxidative demethylation of polymeric lignin via generation of hydroxyl radical. *ACS Chem. Biol.* **13**, 2920–2929 (2018).

136. Rashid, G. M. & Bugg, T. D. Enhanced biocatalytic degradation of lignin using combinations of lignin-degrading enzymes and accessory enzymes. *Catal. Sci. Technol.* **11**, 3568–3577 (2021).
137. Bugg, T. D., Ahmad, M., Hardiman, E. M. & Singh, R. The emerging role for bacteria in lignin degradation and bio-product formation. *Curr. Opin. Biotechnol.* **22**, 394–400 (2011).
138. Kirk, T. K. & Farrell, R. L. Enzymatic "combustion": the microbial degradation of lignin. *Annu. Rev. Microbiol.* **41**, 465–505 (1987).
139. Tien, M. & Kirk, T. K. Lignin-degrading enzyme from the hymenomycete *Phanerochaete chrysosporium* burds. *Science* **221**, 661–663 (1983).
140. Enoki, A. & Gold, M. H. Degradation of the diarylpropane lignin model compound 1-(3,4-diethoxyphenyl)-1,3-dihydroxy-2-(4-methoxyphenyl)-propane and derivatives by the basidiomycete *Phanerochaete chrysosporium*. *Arch. Microbiol.* **132**, 123–130 (1982).
141. Chen, Y. R., Sarkanen, S. & Wang, Y. Y. Lignin-degrading enzyme activities. *Methods Mol. Biol.* **908**, 251–268 (2012).
142. Del Cerro, C. et al. Intracellular pathways for lignin catabolism in white-rot fungi. *Proc. Natl Acad. Sci. USA* **118**, e2017381118 (2021).
143. Shettigar, M. et al. Isolation of the (+)-pinoresinol-mineralizing *Pseudomonas* sp. strain SG-MS2 and elucidation of its catabolic pathway. *Appl. Environ. Microbiol.* **84**, e02531-17 (2018).
144. Fukuhara, Y. et al. Discovery of pinoresinol reductase genes in sphingomonads. *Enzyme Microb. Technol.* **52**, 38–43 (2013).
145. Takahashi, K., Miyake, K., Hishiyama, S., Kamimura, N. & Masai, E. Two novel decarboxylase genes play a key role in the stereospecific catabolism of dehydrodiconiferyl alcohol in *Sphingobium* sp. strain SYK-6. *Environ. Microbiol.* **20**, 1739–1750 (2018).
146. Presley, G. N. et al. Pathway discovery and engineering for cleavage of a β-1 lignin-derived biaryl compound. *Metab. Eng.* **65**, 1–10 (2021).
147. Kato, R. et al. Stereoinversion via alcohol dehydrogenases enables complete catabolism of β-1-type lignin-derived aromatic isomers. *Appl. Environ. Microbiol.* **89**, e0017123 (2023).
148. Kuatsjah, E. et al. Biochemical and structural characterization of a sphingomonad diarylpropane lyase for cofactorless deformylation. *Proc. Natl Acad. Sci. USA* **120**, e2212246120 (2023).
149. Hammel, K. E., Tien, M., Kalyanaraman, B. & Kirk, T. K. Mechanism of oxidative C alpha-C beta cleavage of a lignin model dimer by *Phanerochaete chrysosporium* ligninase. Stoichiometry and involvement of free radicals. *J. Biol. Chem.* **260**, 8348–8353 (1985).
150. Sonoki, T. et al. Coexistence of two different O-demethylation systems in lignin metabolism by *Sphingomonas paucimobilis* SYK-6: cloning and sequencing of the lignin biphenyl-specific O-demethylase (LigX) Gene. *Appl. Environ. Microbiol.* **66**, 2125–2132 (2000).
151. Sheng, X. et al. A combined experimental-theoretical study of the LigW-catalyzed decarboxylation of 5-carboxyvanillate in the metabolic pathway for lignin degradation. *ACS Catal.* **7**, 4968–4974 (2017).
152. Mazurkewich, S., Brott, A. S., Kimber, M. S. & Seah, S. Y. Structural and kinetic characterization of the 4-carboxy-2-hydroxymuconate hydratase from the gallate and protocatechuate 4,5-cleavage pathways of *Pseudomonas putida* KT2440. *J. Biol. Chem.* **291**, 7669–7686 (2016).
153. Hogancamp, T. N., Mabanglo, M. F. & Raushel, F. M. Structure and reaction mechanism of the LigJ hydratase: an enzyme critical for the bacterial degradation of lignin in the protocatechuate 4,5-cleavage pathway. *Biochemistry* **57**, 5841–5850 (2018).
154. Hogancamp, T. N., Cory, S. A., Barondeau, D. P. & Raushel, F. M. Structure and chemical reaction mechanism of LigU, an enzyme that catalyzes an allylic isomerization in the bacterial degradation of lignin. *Biochemistry* **58**, 3494–3503 (2019).
155. Linger, J. G. et al. Lignin valorization through integrated biological funneling and chemical catalysis. *Proc. Natl Acad. Sci. USA* **111**, 12013–12018 (2014).
156. Wu, W., Liu, F. & Singh, S. Toward engineering *E. coli* with an autoregulatory system for lignin valorization. *Proc. Natl Acad. Sci. USA* **115**, 2970–2975 (2018).
157. Chen, Z. & Wan, C. Biological valorization strategies for converting lignin into fuels and chemicals. *Renew. Sustain. Energy Rev.* **73**, 610–621 (2017).
158. Wang, Y., Luo, C. B. & Li, Y. Q. Biofuneling lignin-derived compounds into lipids using a newly isolated *Citricoccus* sp. P2. *Bioresour. Technol.* **387**, 129669 (2023).
159. Johnson, C. W. et al. Enhancing muconic acid production from glucose and lignin-derived aromatic compounds via increased protocatechuate decarboxylase activity. *Metab. Eng. Commun.* **3**, 111–119 (2016).
160. Werner, A. Z. et al. Lignin conversion to β-ketoadipic acid by *Pseudomonas putida* via metabolic engineering and bioprocess development. *Sci. Adv.* **9**, eadj0053 (2023).
161. Picart, P. et al. Multi-step biocatalytic depolymerization of lignin. *Appl. Microbiol. Biotechnol.* **101**, 6277–6287 (2017).
162. Picart, P. et al. Assessing lignin types to screen novel biomass-degrading microbial strains: synthetic lignin as useful carbon source. *ACS Sustain. Chem. Eng.* **4**, 651–655 (2016).
163. Picart, P., de Maria, P. D. & Schallmey, A. From gene to biorefinery: microbial β-etherases as promising biocatalysts for lignin valorization. *Front. Microbiol.* **6**, 916 (2015).
164. Picart, P., Sevenich, M., Domínguez de María, P. & Schallmey, A. Exploring glutathione lyases as biocatalysts: paving the way for enzymatic lignin depolymerization and future stereoselective applications. *Green Chem.* **17**, 4931–4940 (2015).
165. Picart, P. et al. From gene towards selective biomass valorization: bacterial β-etherases with catalytic activity on lignin-like polymers. *ChemSusChem* **7**, 3164–3171 (2014).
166. Vom Stein, T. et al. From biomass to feedstock: one-step fractionation of lignocellulose components by the selective organic acid-catalyzed depolymerization of hemicellulose in a biphasic system. *Green Chem.* **13**, 1772 (2011).
167. Grande, P. M. et al. Fractionation of lignocellulosic biomass using the OrganoCat process. *Green Chem.* **17**, 3533–3539 (2015).
168. Brandner, D. G. et al. Flow-through solvolysis enables production of native-like lignin from biomass. *Green Chem.* **23**, 5437–5441 (2021).
169. Alherech, M. et al. From lignin to valuable aromatic chemicals: lignin depolymerization and monomer separation via centrifugal partition chromatography. *ACS Cent. Sci.* **7**, 1831–1837 (2021).
170. Yang, X. & Wang, D. Photocatalysis: from fundamental principles to materials and applications. *ACS Appl. Energy Mater.* **1**, 6657–6693 (2018).
171. Xiang, Z. et al. Photocatalytic conversion of lignin into chemicals and fuels. *ChemSusChem* **13**, 4199–4213 (2020).
172. Murnaghan, C. W. et al. Toward the photocatalytic valorization of lignin: conversion of a model lignin hexamer with multiple functionalities. *ACS Sustain. Chem. Eng.* **10**, 12107–12116 (2022).

Acknowledgements

This work was authored in part by the National Renewable Energy Laboratory, operated by the Alliance for Sustainable Energy, LLC, for the US Department of Energy (DOE) under Contract No. DE-AC36-08GO28308. Funding to C.T.P., E.T.O., J.Z., Y.R.L. and G.T.B. was provided by the US DOE, Office of Energy Efficiency and Renewable Energy, Bioenergy Technologies Office. For J.Z., Y.R.L. and G.T.B., this material is also based upon work supported by the Center for Bioenergy Innovation, US DOE, Office of Science, Biological and Environmental Research Program under Award Number ERKP886. Contributions by S.S.S. were supported by the US DOE, Office of Basic Energy Sciences, under award no. DEFG02-05ER15690. The views expressed in the article do not necessarily represent the views of the DOE or the US Government. The US Government retains and the publisher, by accepting the article for publication, acknowledges that the US Government retains a nonexclusive, paid-up, irrevocable, worldwide license to publish or reproduce the published form of this work, or allow others to do so, for US Government purposes.

Author contributions

C.T.P., E.T.O. and J.Z. wrote the first draft of the paper, which was edited and approved by all authors.

Competing interests

The authors declare no competing interests.

Additional information

Supplementary information The online version contains supplementary material available at https://doi.org/10.1038/s41570-024-00652-9.

Peer review information *Nature Reviews Chemistry* thanks the anonymous reviewers for their contribution to the peer review of this work.